

Detailed energy (mass) budget of the Universe

THE COSMIC ENERGY INVENTORY

MASATAKA FUKUGITA

Institute for Advanced Study, Einstein Drive, Princeton, NJ 08540; and Institute for Cosmic Ray Research,
University of Tokyo, Kashiwa 277-8582, Japan

AND

P. J. E. PEEBLES

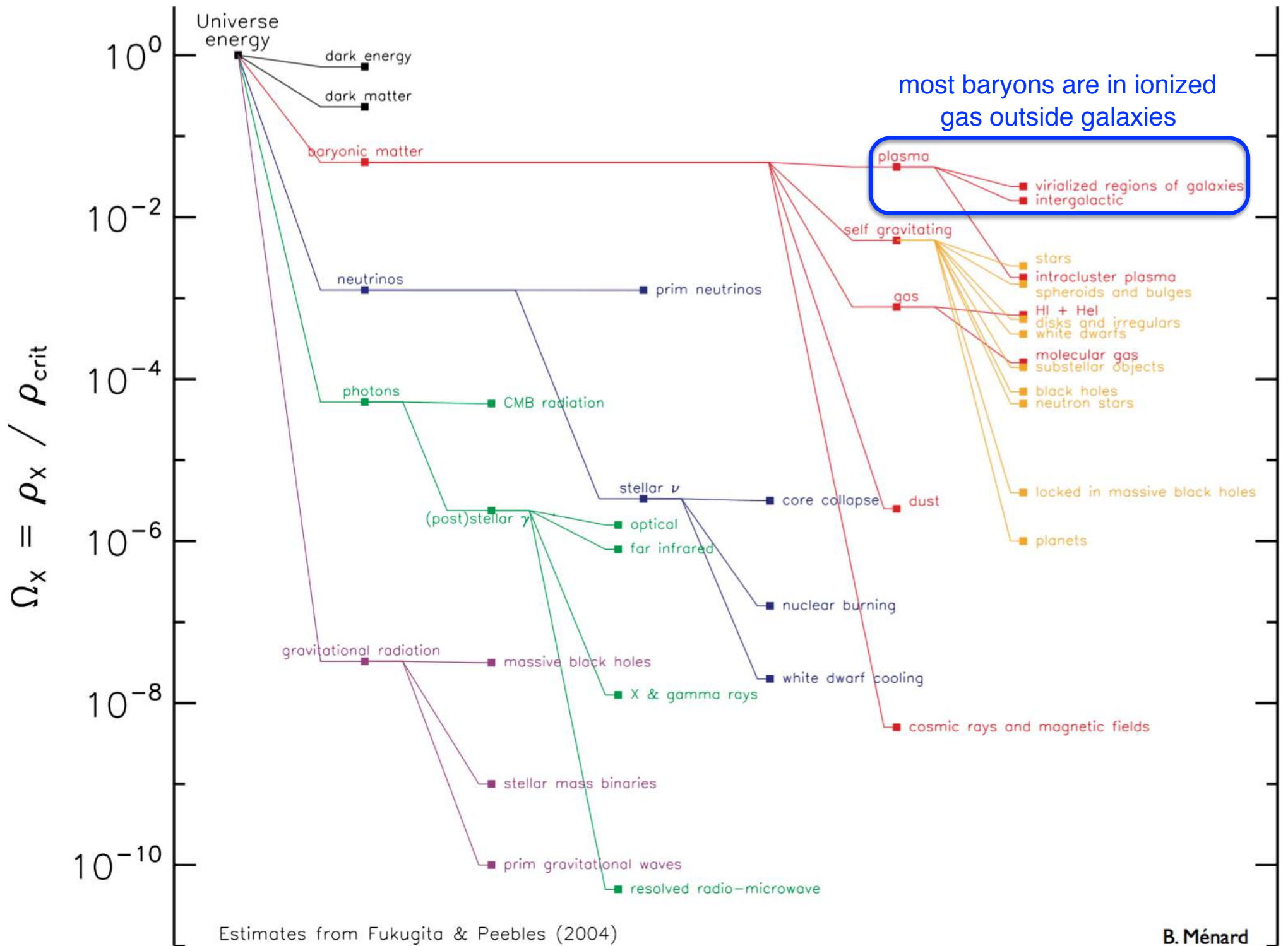
Joseph Henry Laboratories, Princeton University, Jadwin Hall, P.O. Box 708, Princeton, NJ 08544

Received 2004 June 3; accepted 2004 August 9

ABSTRACT

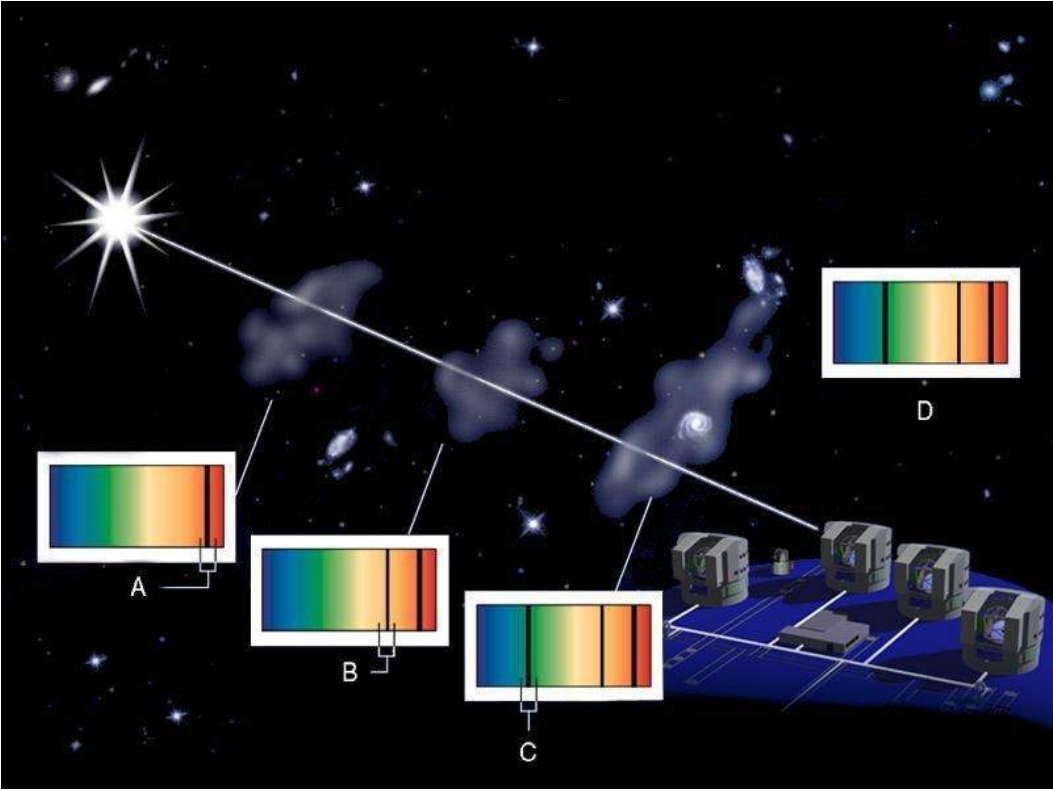
We present an **inventory of the cosmic mean densities of energy associated with all the known states of matter** and radiation at the present epoch. The observational and theoretical bases for the inventory have become rich enough to allow estimates with observational support for the densities of energy in some 40 forms. The result is a global portrait of the effects of the physical processes of cosmic evolution.

Subject heading: cosmology: miscellaneous

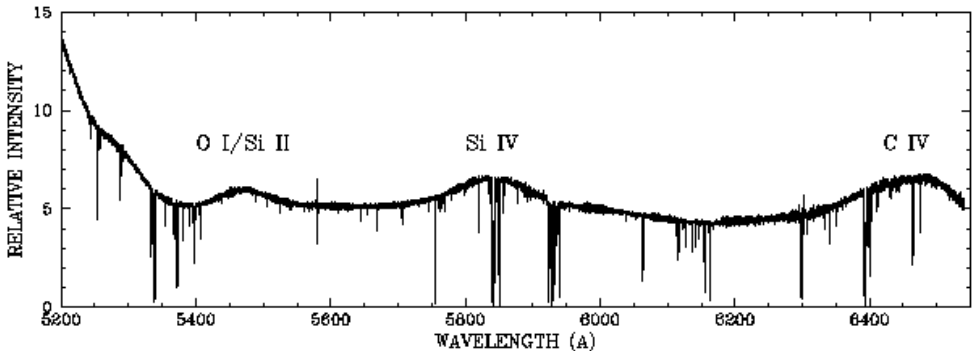
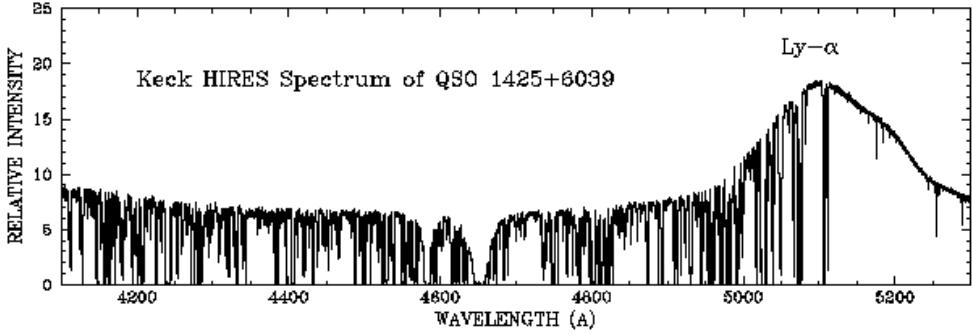


Intergalactic baryons

Quasar absorption lines

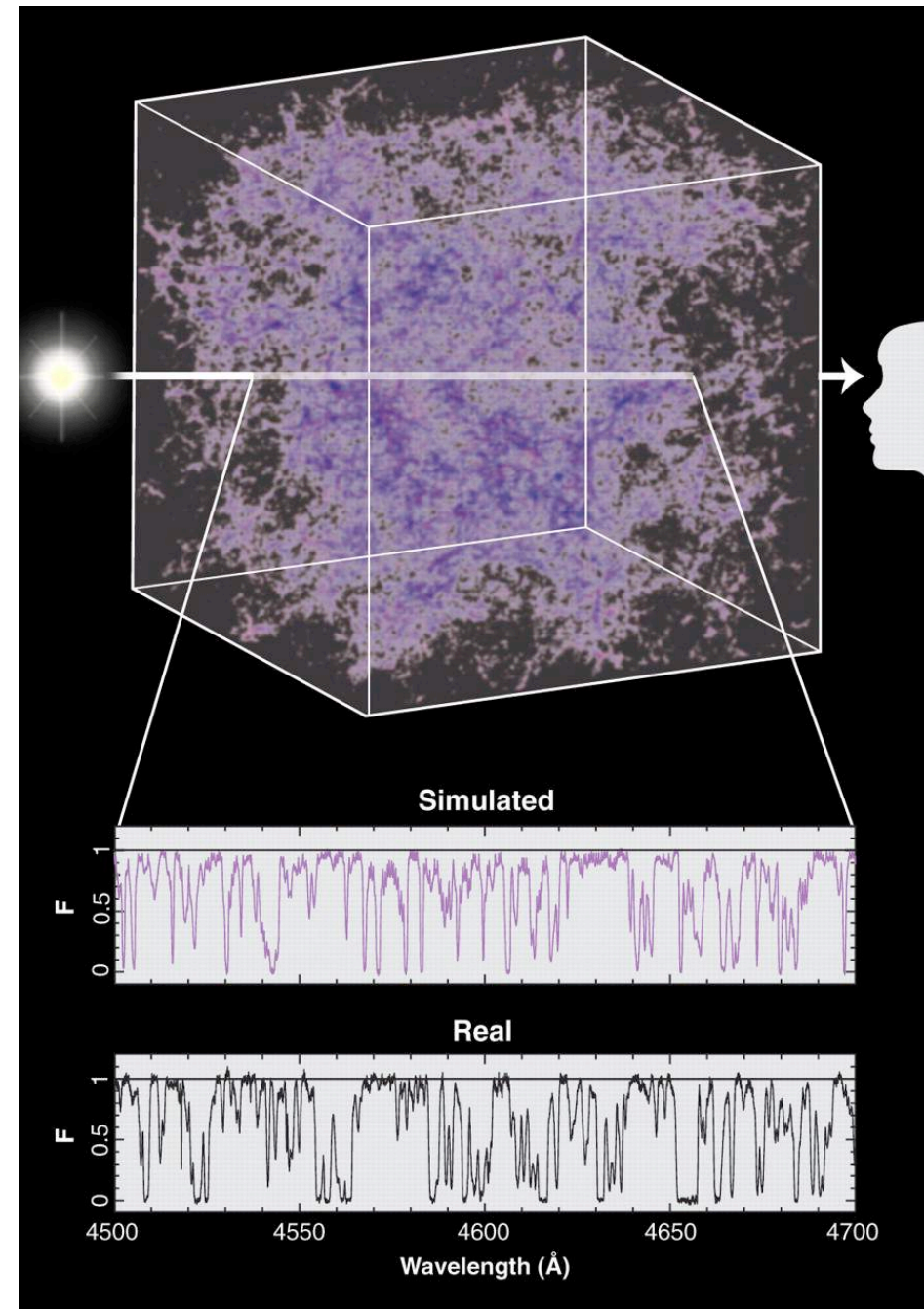


$Z_{QSO} = 3.18$



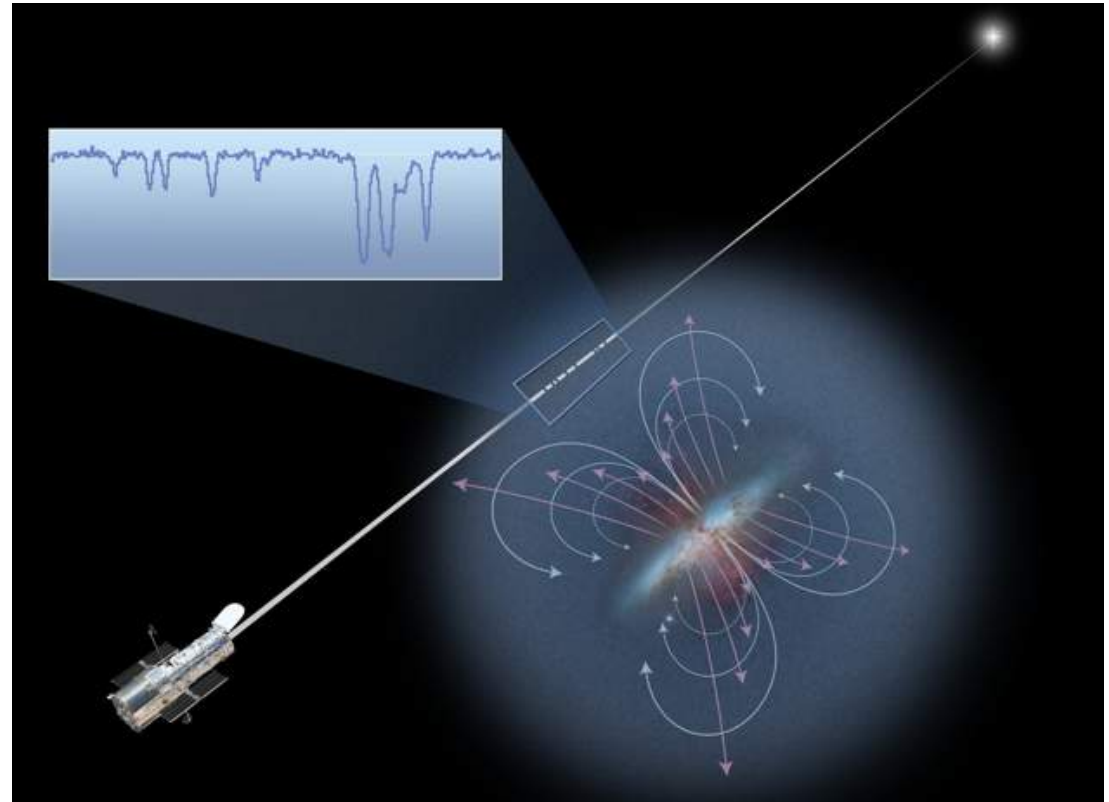
The Ly α forest as a probe of intergalactic gas

- The space between galaxies is filled with baryons
- See in hydrogen Ly α absorption in spectra of distant quasars
- High-redshift ($z \sim 2-4$) Ly α forest observations are consistent with the BBN baryon abundance, i.e. consistent with most baryons being intergalactic



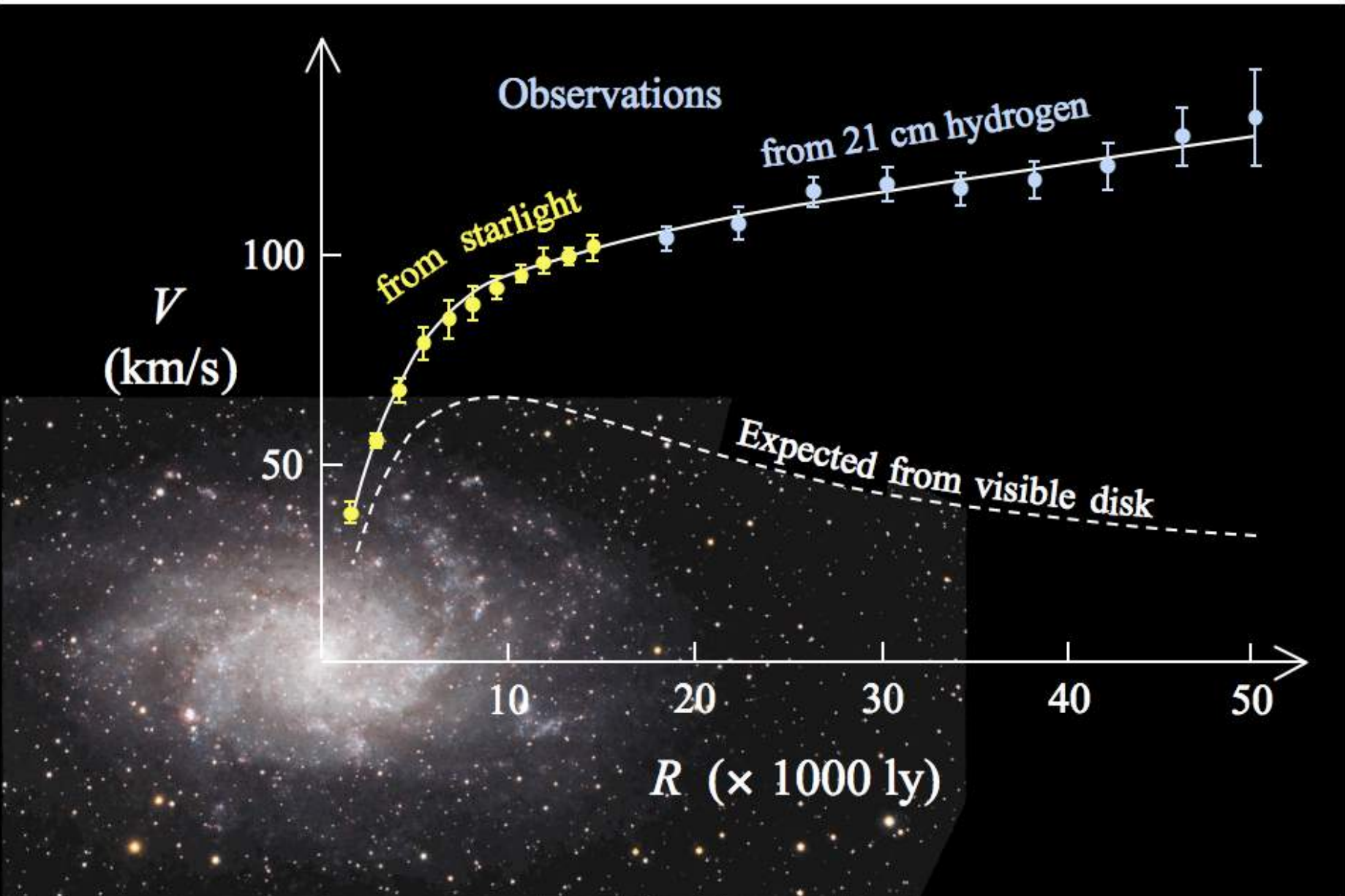
Gas in halos of galaxies (circum-galactic medium)

- Galaxy growth is regulated by mass exchanges with the intergalactic medium
 - ▶ inflows fuel star formation & black hole growth
 - ▶ feedback from stars and black holes drive powerful outflows
- These baryons are faint: absorption spectroscopy currently gives best constraints

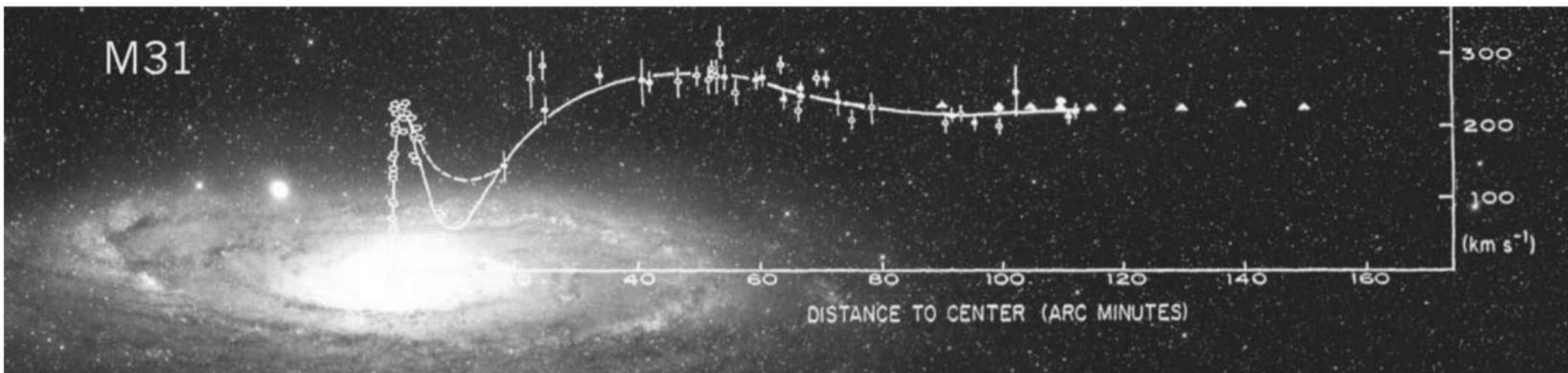


Galaxy rotation curves

Galaxy rotation curves: evidence for dark matter



M33 rotation curve from http://en.wikipedia.org/wiki/Galaxy_rotation_curve



The M31 major axis mean optical radial velocities and the rotation curve,⁴ $r < 120$ arcmin, superposed on the M31 image from the Palomar Sky Survey. Velocities from radio observations⁵ are indicated by triangles, $90 < r < 150$ arcmin. Rotation velocities remain flat well beyond the optical galaxy, implying that the M31 cumulative mass rises linearly with radius. (Image by Rubin and Janice Dunlap.)



Vera Rubin pioneered measurements of galaxy rotation curves. Starting with her Rubin & Kent (1970) paper on the rotation curve of M31, her work provided compelling evidence for extended halos of dark matter around galaxies.

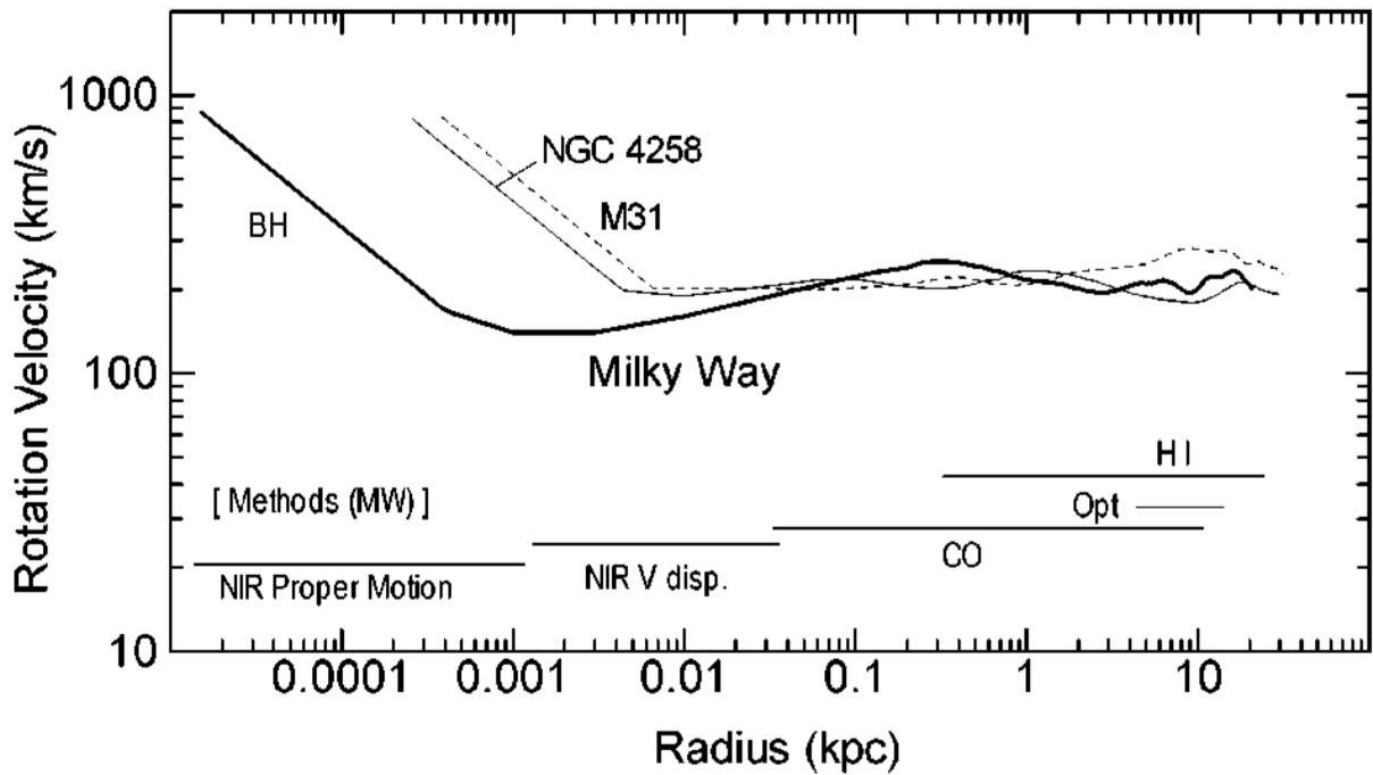


Figure 3 Logarithmic rotation curves of the Milky Way (thick line), NGC 4258 (thin line), and M31 (dashed line). Innermost rotation velocities are Keplerian velocities calculated for massive black holes. Observational methods for the Milky Way (horizontal lines).

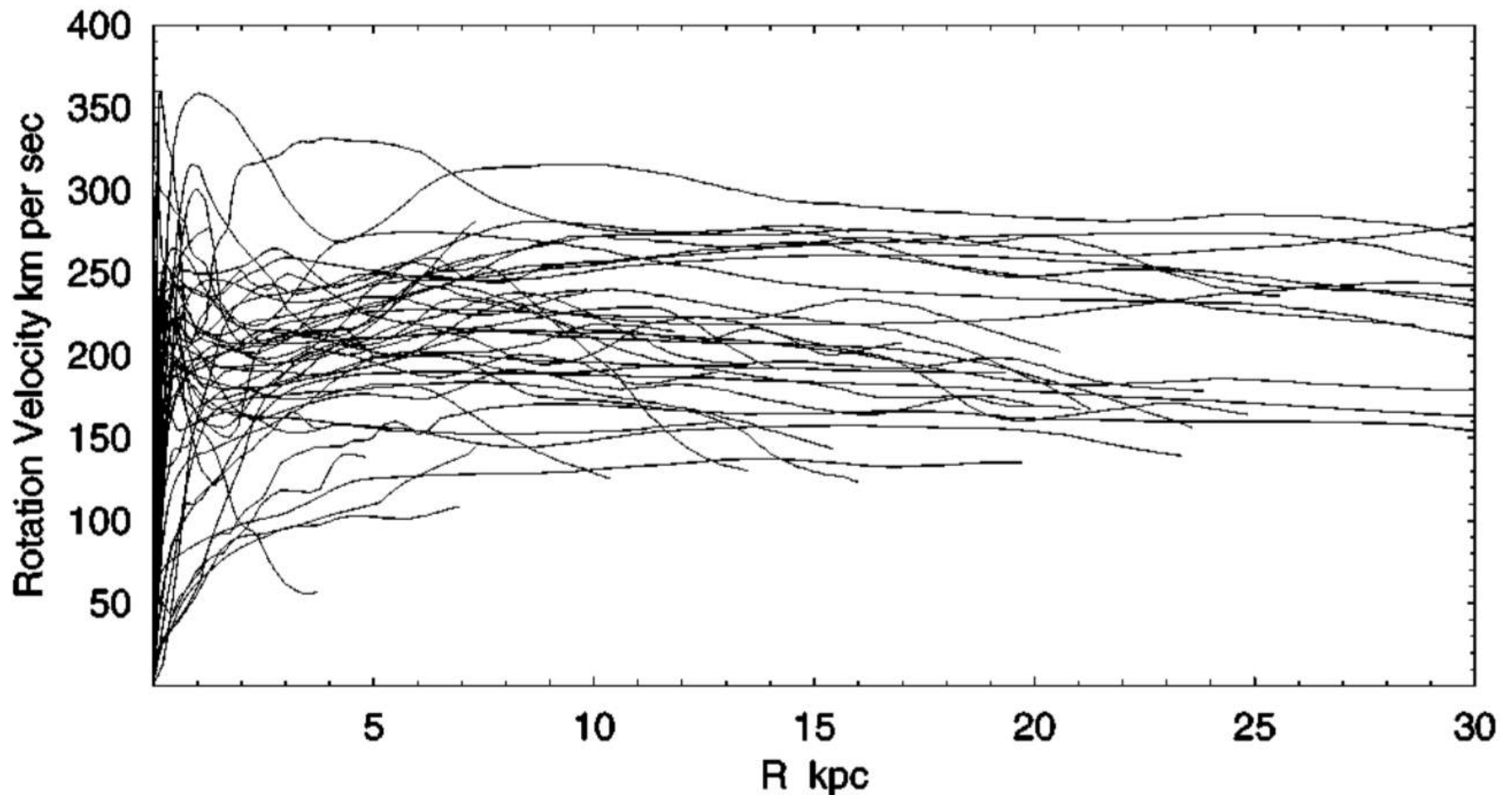


Figure 4 Rotation curves of **spiral galaxies** obtained by combining CO data for the central regions, optical for disks, and HI for outer disk and halo (Sofue et al. 1999a).

Digression:
Rotation curves for disk mass
distributions

(rather than spherically-symmetrically
distributed — Newton's theorem does *not*
apply)

Example for razor-thin exponential disk

Mass distribution: $\Sigma(R) = \Sigma_0 e^{-R/R_d}$

Potential obtained by solving Poisson's eq:

$$\begin{aligned}\Phi(R, 0) &= -4G\Sigma_0 \int_0^R da \frac{aK_1(a/R_d)}{\sqrt{R^2 - a^2}} \\ &= -\pi G\Sigma_0 R [I_0(y)K_1(y) - I_1(y)K_0(y)] \quad y \equiv \frac{R}{2R_d}\end{aligned}$$

↑ ↑
modified Bessel functions

Rotation curve:

$$v_c^2(R) = R \frac{\partial \Phi}{\partial R} = 4\pi G\Sigma_0 R_d y^2 [I_0(y)K_0(y) - I_1(y)K_1(y)]$$

Applying Newton's theorem to disk is not strictly correct, but the approximation is good to $\sim 15\%$

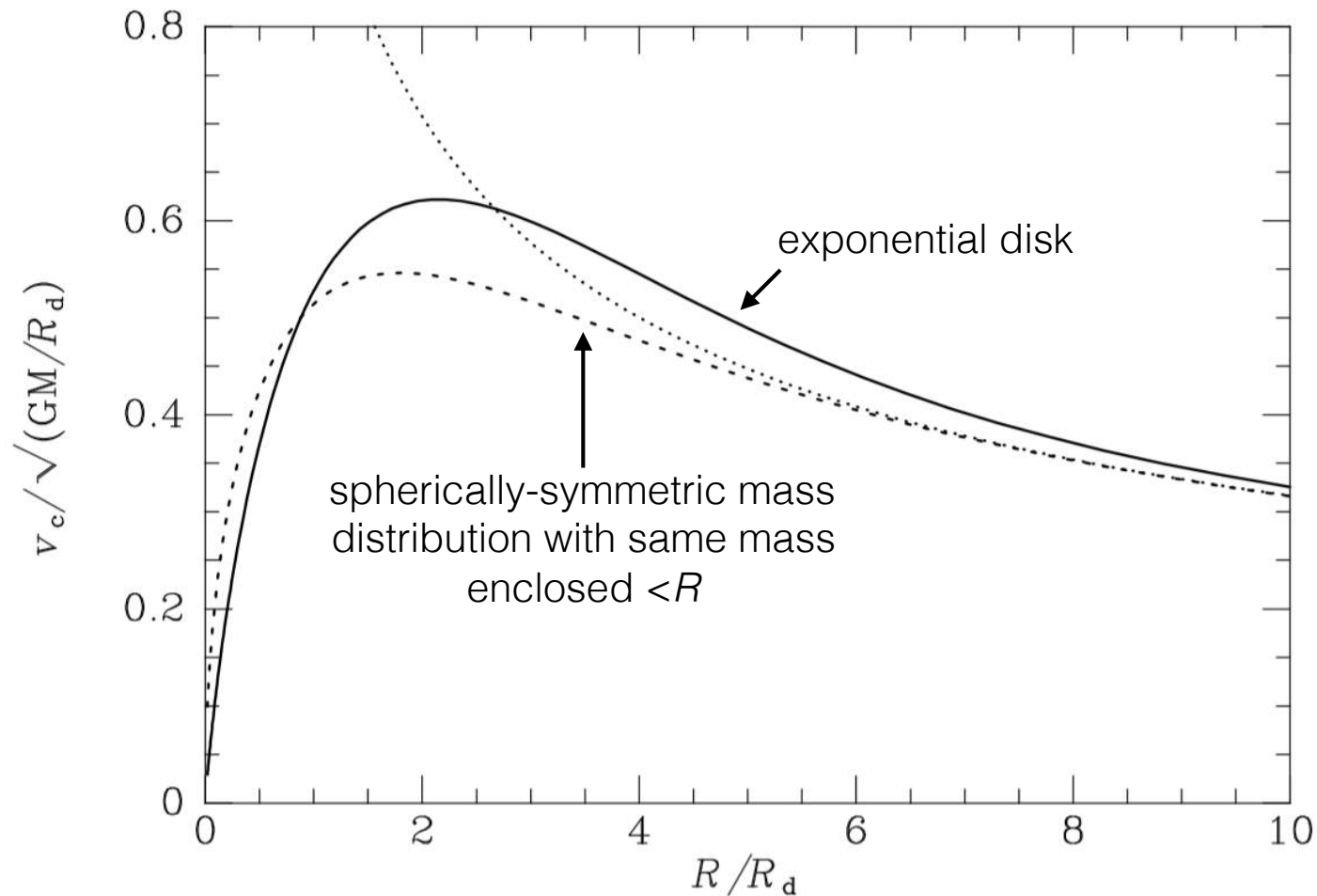


Figure 2.17 The circular-speed curves of: an exponential disk (full curve); a point with the same total mass (dotted curve); the spherical body for which $M(r)$ is given by equation (2.166) (dashed curve).

Dark matter in galaxy clusters

Coma galaxy cluster in optical



~2,000 galaxies total

Coma cluster in x-rays

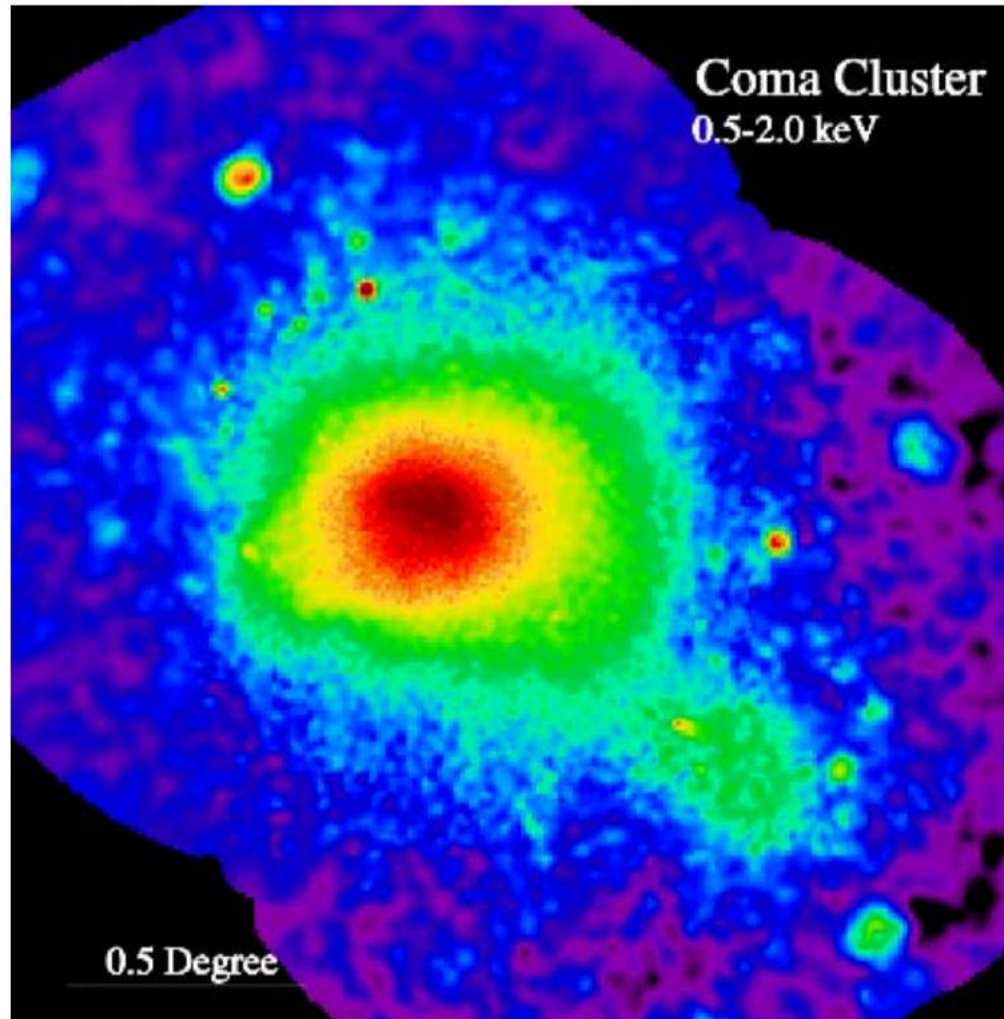


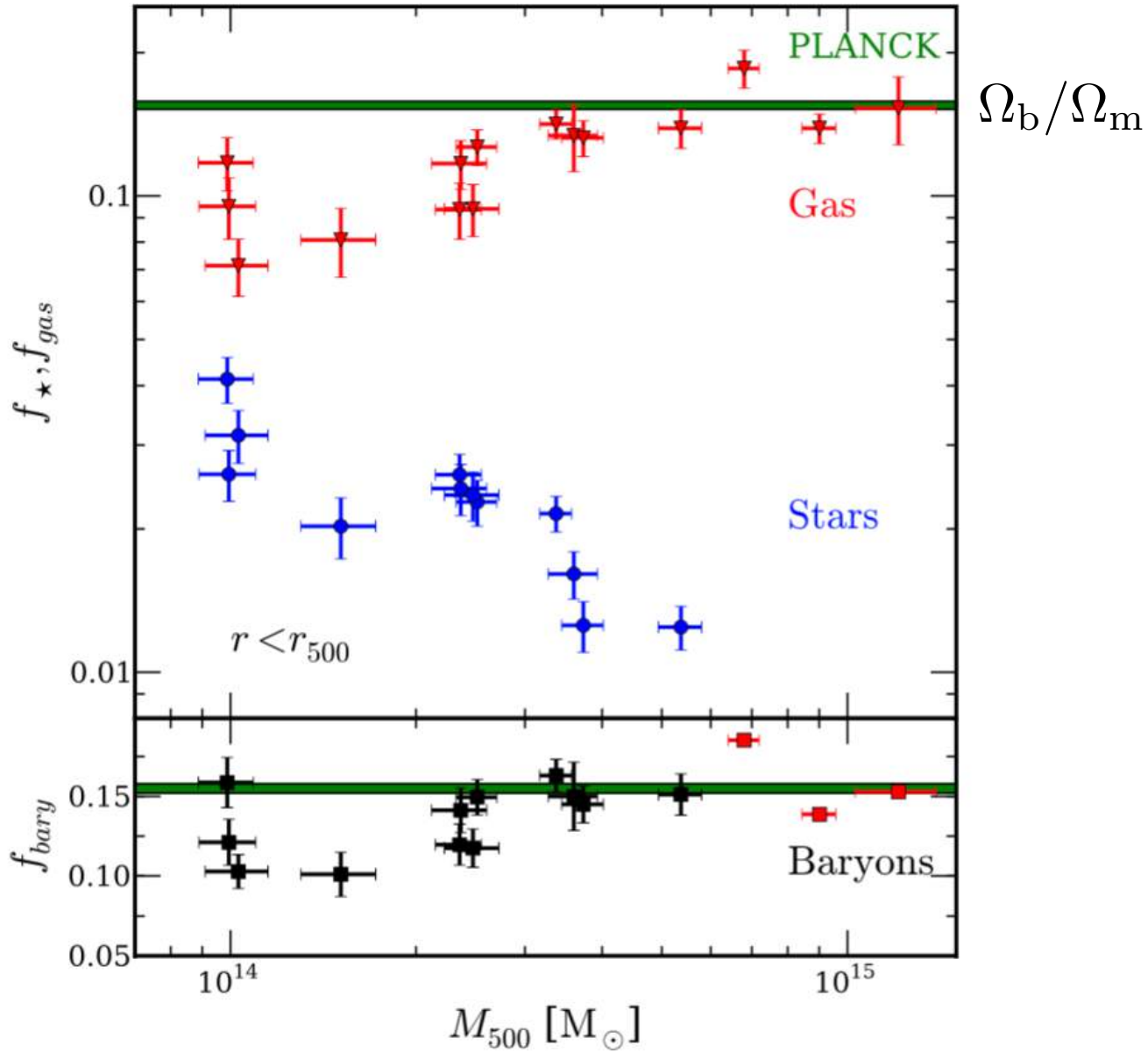
Figure 2. An x-ray image of the Coma cluster obtained with the ROSAT satellite, showing both the main cluster and the NGC4839 group to the south-west. (Credit: S L Snowden, High Energy Astrophysics Science Archive Research Center, NASA.)

Coma cluster: x-rays on top of optical



Most baryons in galaxy clusters are in hot gas, not stars — but not enough gas to account for all mass

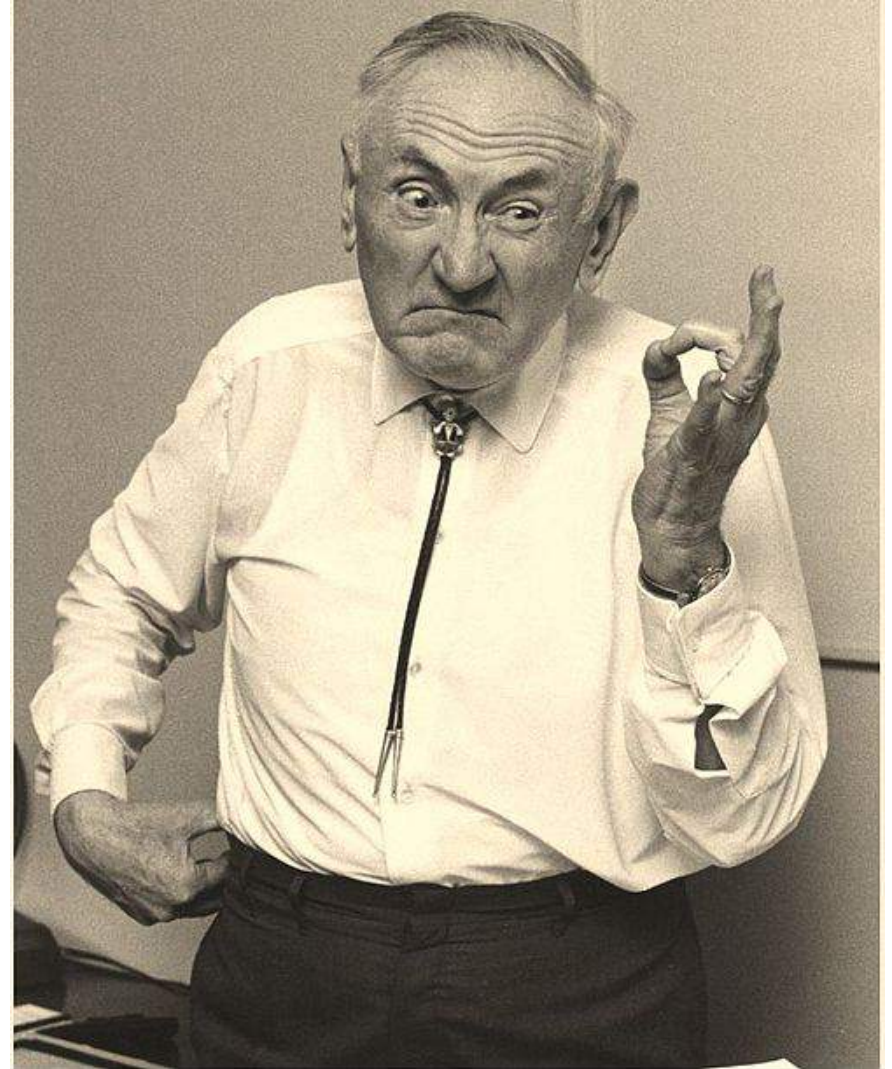
mass fractions in stars and gas



mass enclosed within $500\rho_{crit}$

Fritz Zwicky (1898-1974)

- First observational evidence for dark matter by applying virial theorem to galaxy clusters (1933)
- Coined term 'supernovae' and predicted that they produce neutron stars and cosmic rays (1933)
- Posited in 1937 that galaxy clusters could act as gravitational lenses (first observed in 1979)
- Produced many catalogs of observed galaxies and galaxy clusters (1961-1971)
- Developed some of the earliest jet engines and holds over 50 patents
- ...



CATALOGUE OF SELECTED COMPACT GALAXIES AND OF POST-ERUPTIVE GALAXIES

F. Zwicky (1971)

INTRODUCTION

...The naivety of some of the theoreticians, at all times, is really appalling. As a shining example of a most deluded individual we need only quote the high pope of American Astronomy, one Henry Norris Russell, ...

...the most renowned observational astronomers in the 1930's also made claims that now have been proved to be completely erroneous...

... E. P. Hubble, W. Baade and the sycophants among their young assistants were thus in a position to doctor their observational data, to hide their shortcomings and to make the majority of the astronomers accept and believe in some of their most prejudicial and erroneous presentations and interpretations of facts.

Thus it was the fate of astronomy ... to be again and again thrown for a loop by some moguls of the respective hierarchies. To this the useless trash in the bulging astronomical journals furnishes vivid testimony.

...useful to recall some of the major absurdities that were promulgated about galaxies, clusters of galaxies and other cosmic objects by the high priests of astronomy during the past few decades.

It must be emphasized right at the outset that no one, with the exception of the author has ever clearly stated what a galaxy is, an omission that no doubt will not only baffle every thinking layman but will in particular be judged ludicrous by any true methodologist or professional in morphological research...

As a consequence some of the most absurd and untenable definitions of quasars, quasistellar objects, "interlopers" have been introduced by A. Sandage, M. Schmidt and others to which we shall return later on.

Some of the most glaringly incorrect conclusions drawn by E. P. Hubble and W. Baade that stubbornly persisted in the minds of most astronomers for decades are the following...

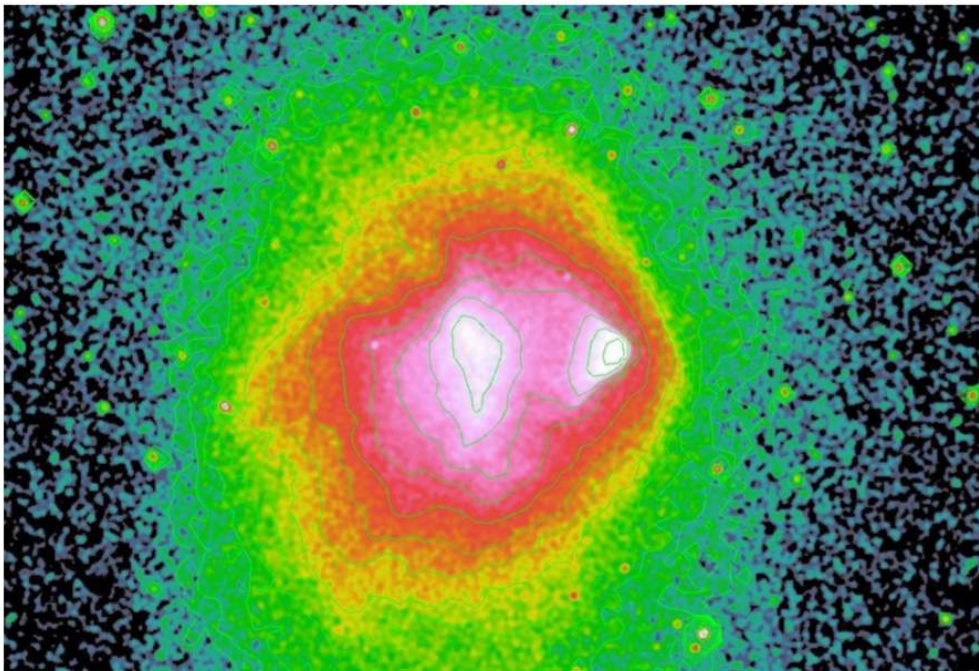
Bullet cluster: more evidence for dark matter



- ▶ two clusters that recently collided
- ▶ gravitational mass traced by weak lensing (blue)
- ▶ gas (pink) stuck in middle

Simulation of merging galaxy clusters matches Bullet cluster properties reasonably well

Observed Bullet cluster x-rays



Simulated Bullet cluster x-rays

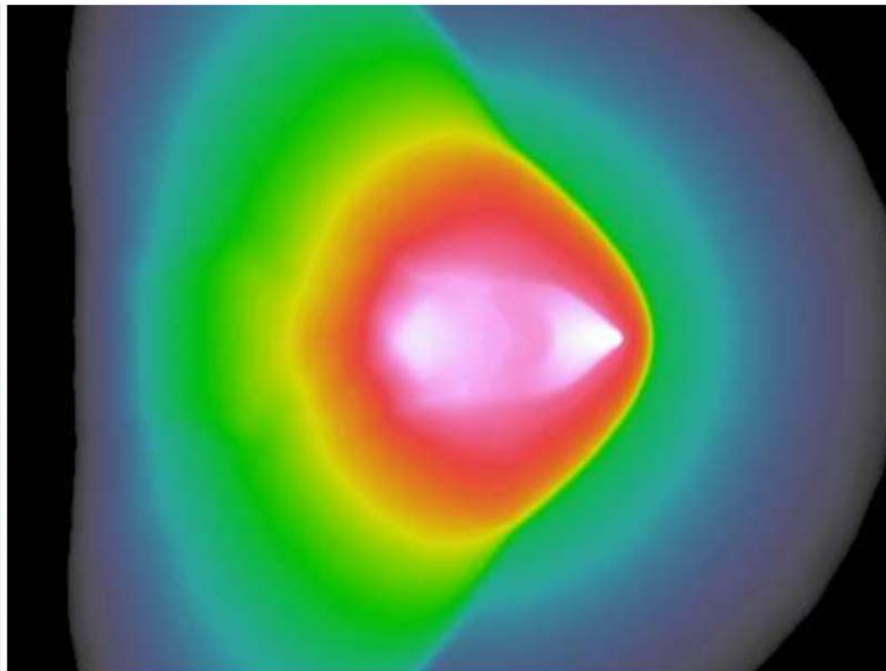
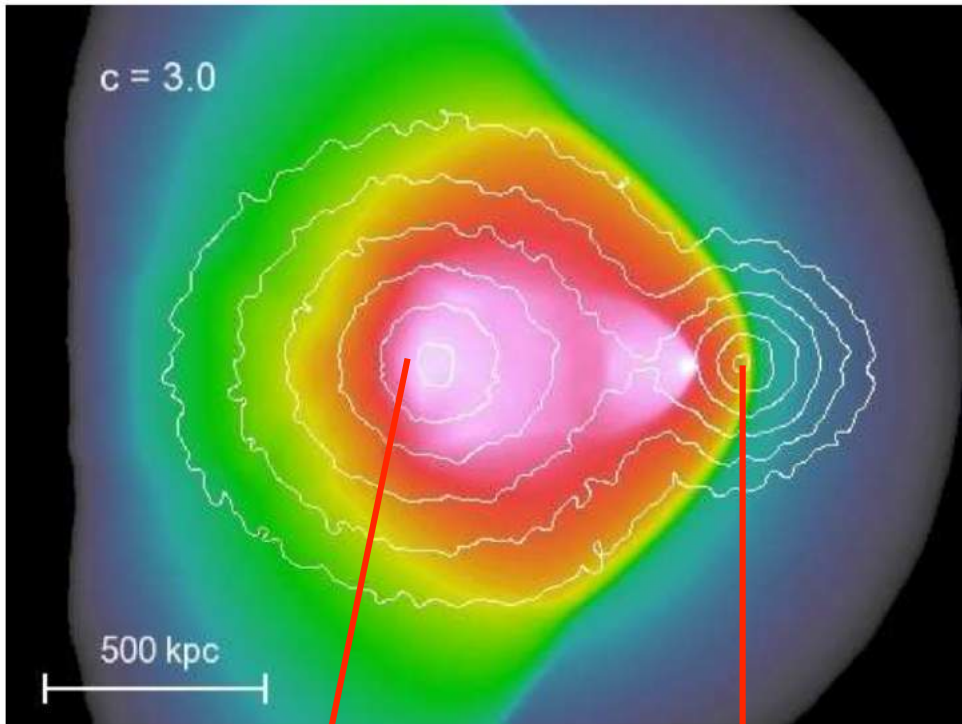


FIG. 2.— X-ray surface brightness of 1E0657–56 observed with Chandra (left). Clearly visible are two X-ray peaks. The wedge-like structure on the right associated with the ‘bullet’ is bounded by a sharp contact discontinuity, which is interpreted as a cold front. The prominent bow shock in front demonstrates that the subcluster is moving to the right with high velocity. The panel on the right-hand side shows the X-ray surface brightness in one of our merger simulations, roughly drawn on the same scale and with similar dynamic range in the color table.

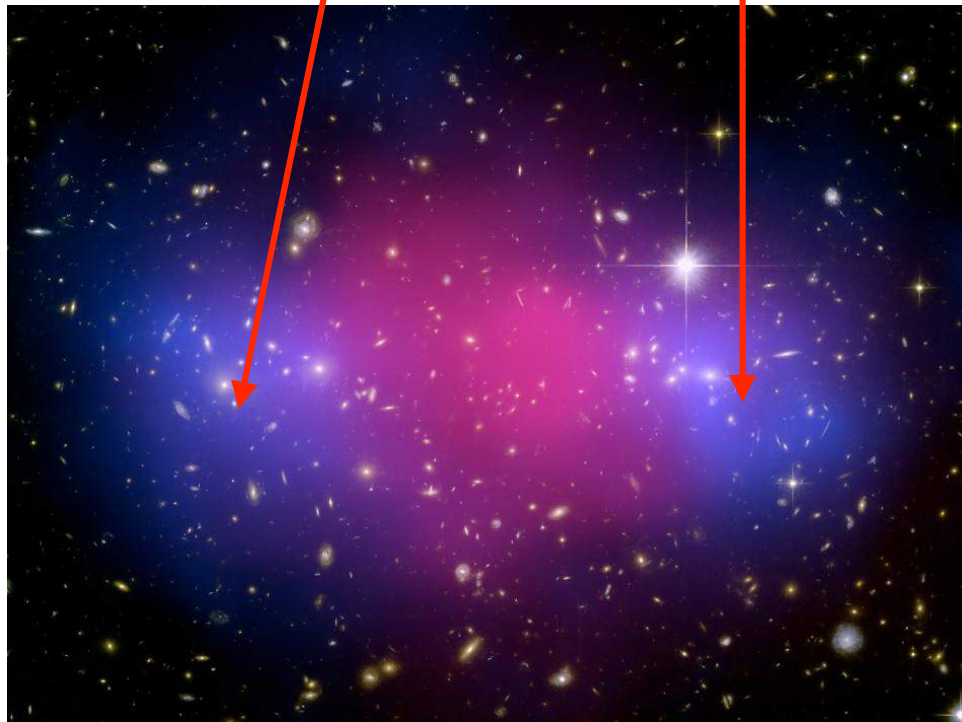
1:10 mass ratio collision at $\sim 2,600$ km/s



Simulated Bullet

Contours: *collisionless* dark matter-dominated mass

Color map: x-ray gas



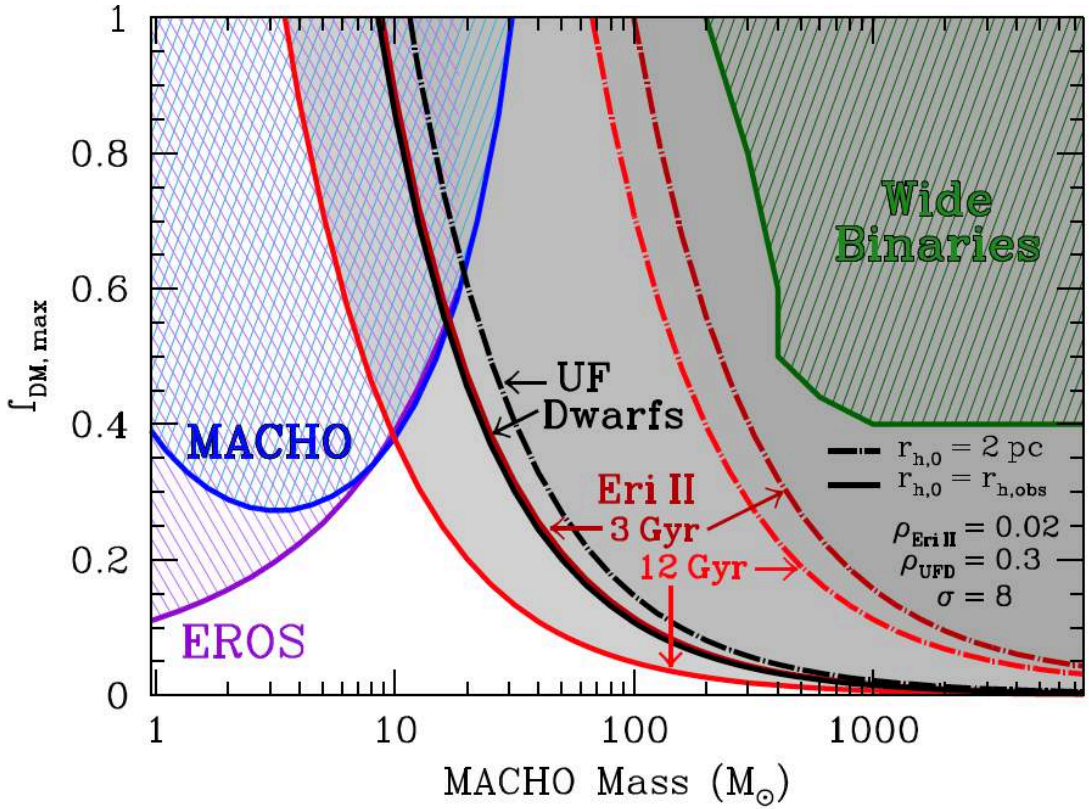
Observed Bullet

Blue: total mass measured using gravitational lensing

Pink: x-ray gas

More on gravitational lensing

MACHO constraints from microlensing (+ other constraints from dynamics)

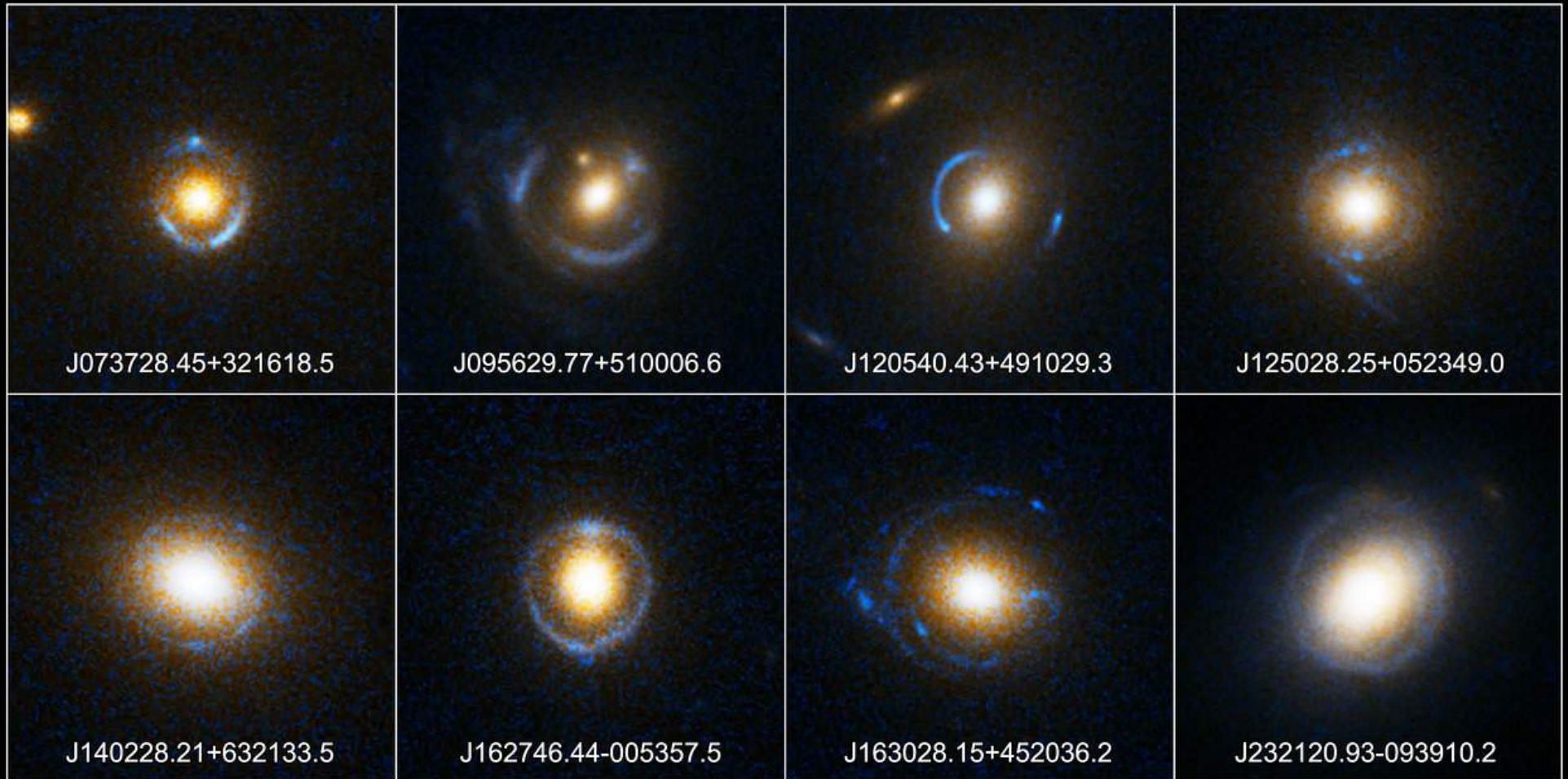


Maximum fraction of the Milky Way's dark halo mass that can be MACHOs

- blue hatched: excluded by microlensing
- other gray/hatched regions: excluded by dynamical considerations (observed stellar structures could not last long if the dark matter were MACHOs)

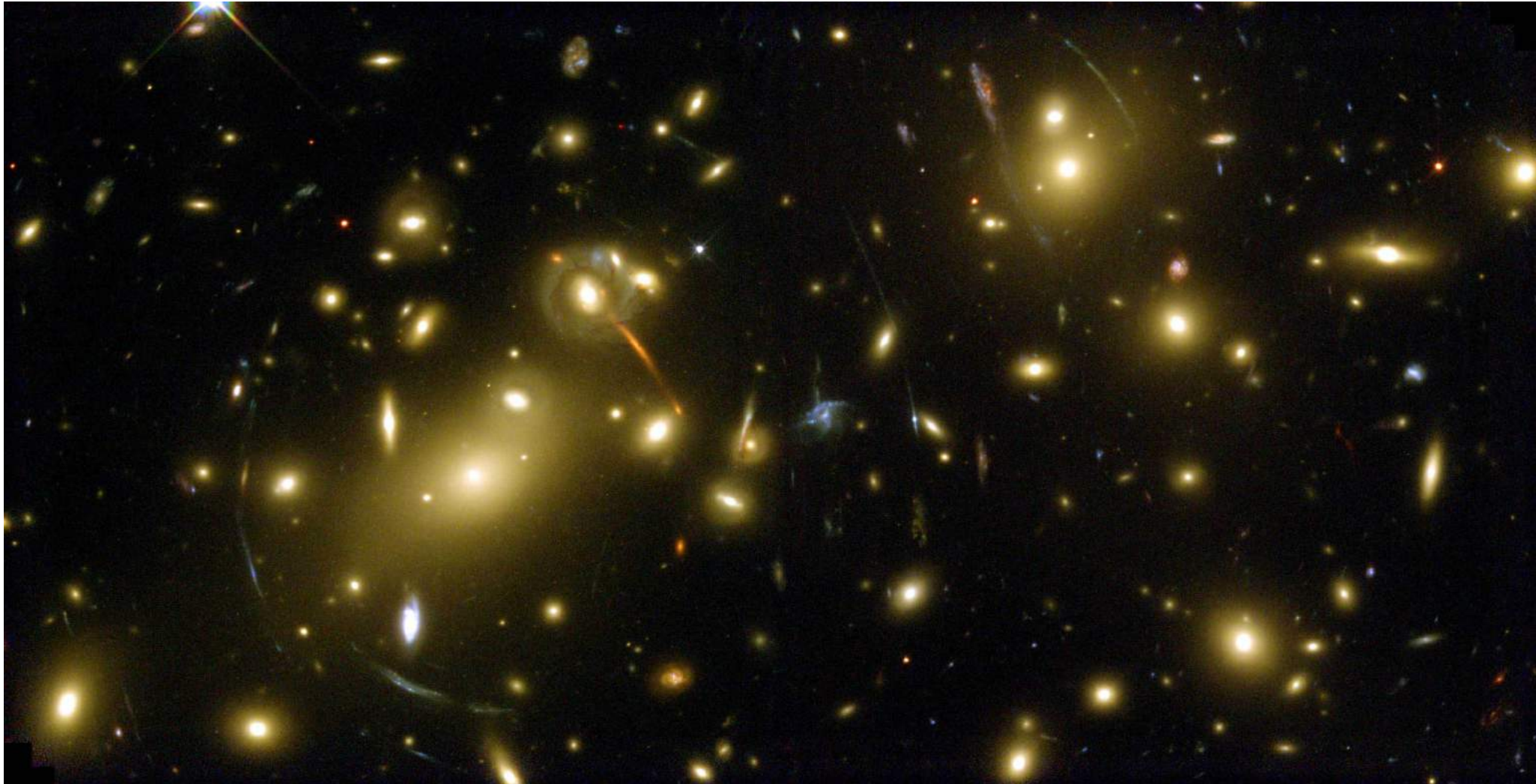
Figure 4. Constraints on MACHO dark matter from microlensing (blue and purple; Alcock et al. 2001; Tisserand et al. 2007) and wide Galactic binaries (green; Quinn et al. 2009), shown together with the constraints from the survival of compact ultra-faint dwarf galaxies and the star cluster in Eridanus II. I conservatively adopt a dark matter density of $0.02 M_{\odot} \text{pc}^{-3}$ in Eri II and $0.3 M_{\odot} \text{pc}^{-3}$ in the ultra-faint dwarfs, assume a three-dimensional velocity dispersion $\sigma = 8 \text{ km s}^{-1}$, and use two definitions of the heating timescale. A low-density halo and initially compact cluster weaken the constraints from Eri II. Even in this case, assuming dark matter halos to have the properties that are currently inferred, MACHO dark matter is excluded for all MACHO masses $\gtrsim 10^{-7} M_{\odot}$.

Einstein rings around elliptical galaxies



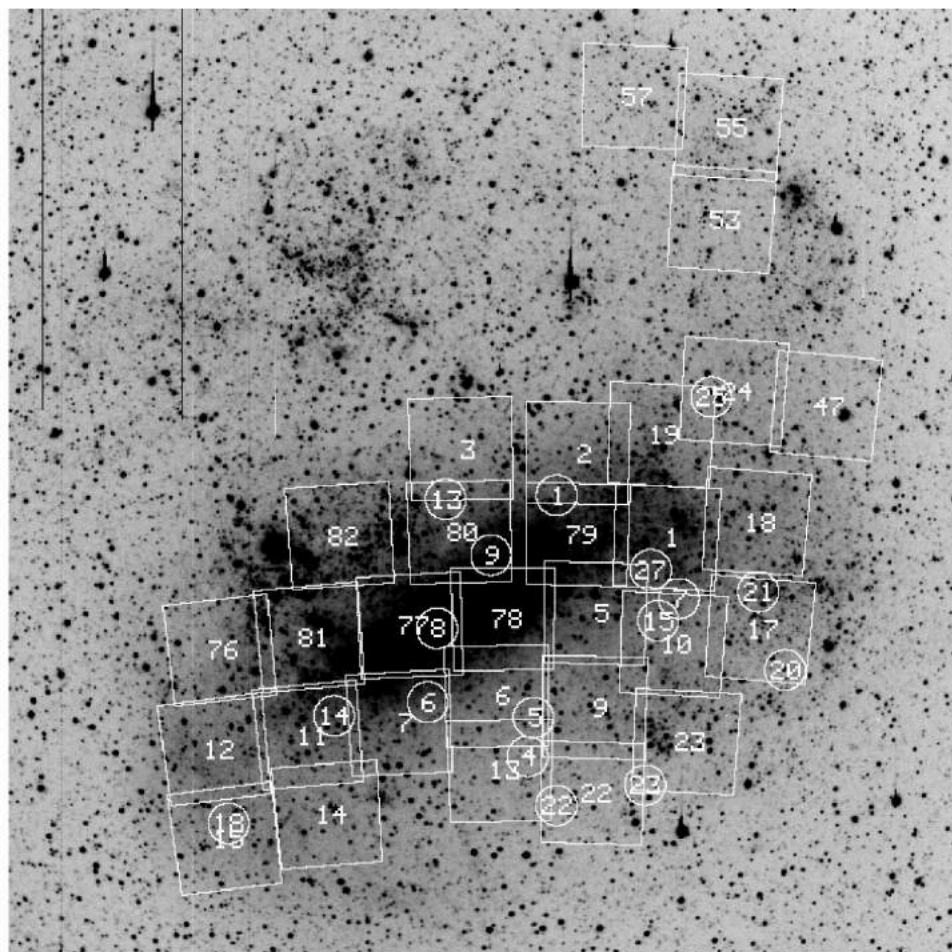
Einstein Ring Gravitational Lenses
Hubble Space Telescope • Advanced Camera for Surveys

Strong lensing arcs in galaxy clusters



More on MACHO project

Observed LMC fields



Example microlensing candidate events

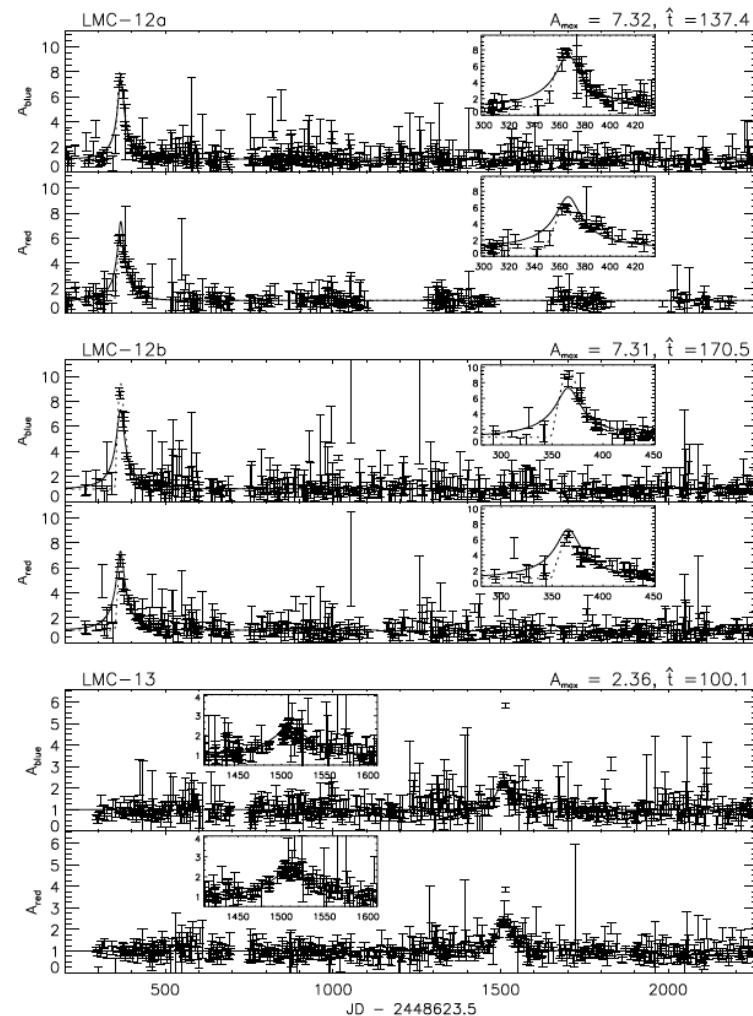
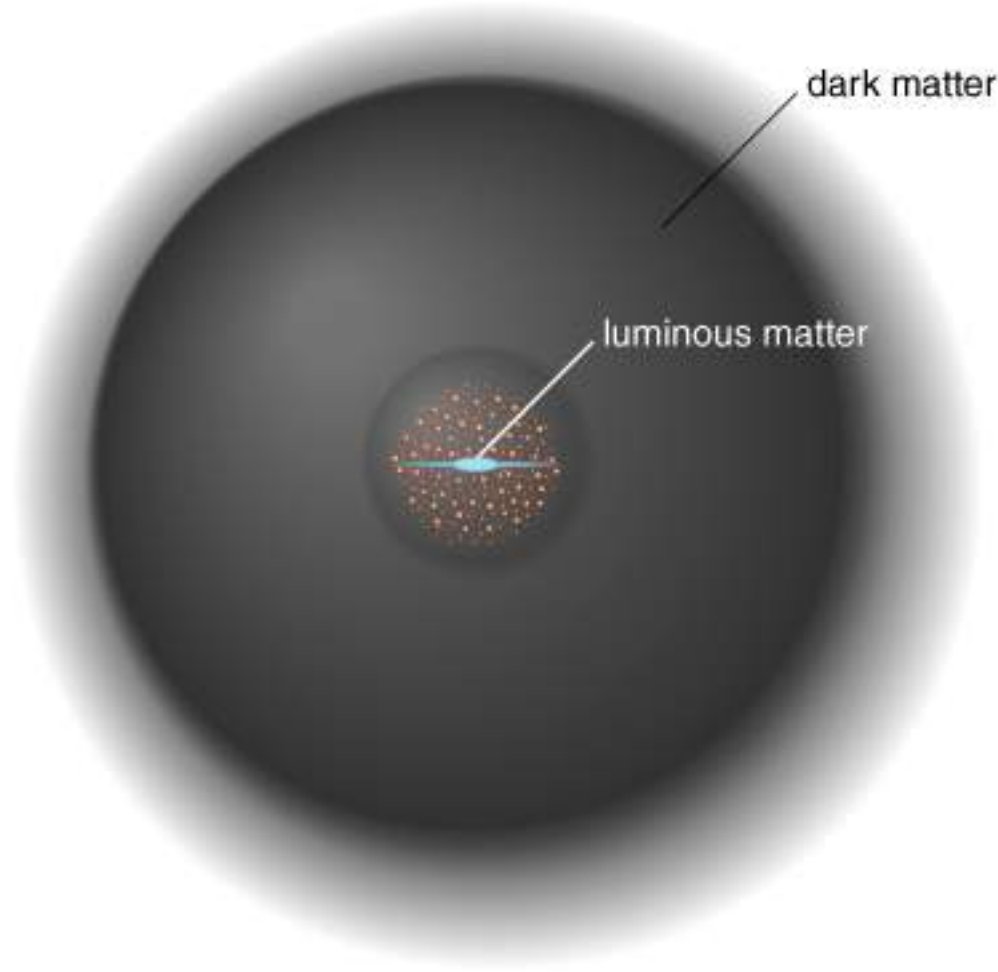


FIG. 1.—R-band image of the LMC, 8°2 on the side (G. Bothun 1997, private communication), showing the locations of the 30 MACHO fields used here. Also shown are the locations of the 17 microlensing candidates discussed in the text. See the electronic edition of the Journal for a color version of this figure.

- 5.7 years of photometry for 11.9 million stars
- 13-17 microlensing events detected on timescales 34-230 days
- there are microlensing “MACHOs” (stellar remnants, etc.) but they are too few by a factor ~ 5 to explain the dark matter

Dark matter halos

Dark halos are much larger than galaxies



E.g., Milky Way:

- scale length of stellar disk $R_{s,\star} \sim \text{few kpc}$
- virial radius of halo

$$R_{200c} \sim 200 \text{ kpc}$$

because baryons can radiate away their energy and condense but dark matter cannot, so is supported in larger structures by internal kinetic energy

Quantitative relationship between galaxy and halo sizes

Can use *abundance matching*
(most massive galaxies in most
massive halos) to connect galaxy
to halo properties

$$\text{At } z=0, r_{1/2} \approx 0.015 R_{200}$$

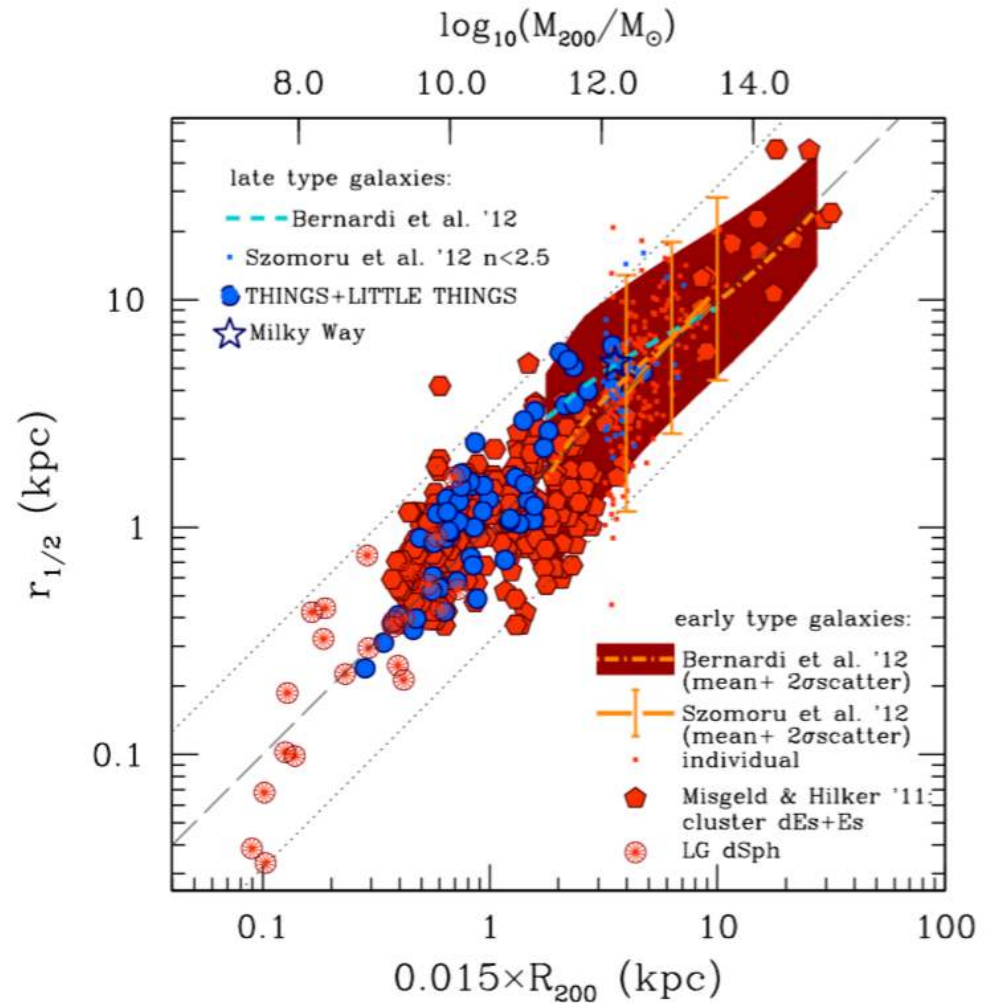
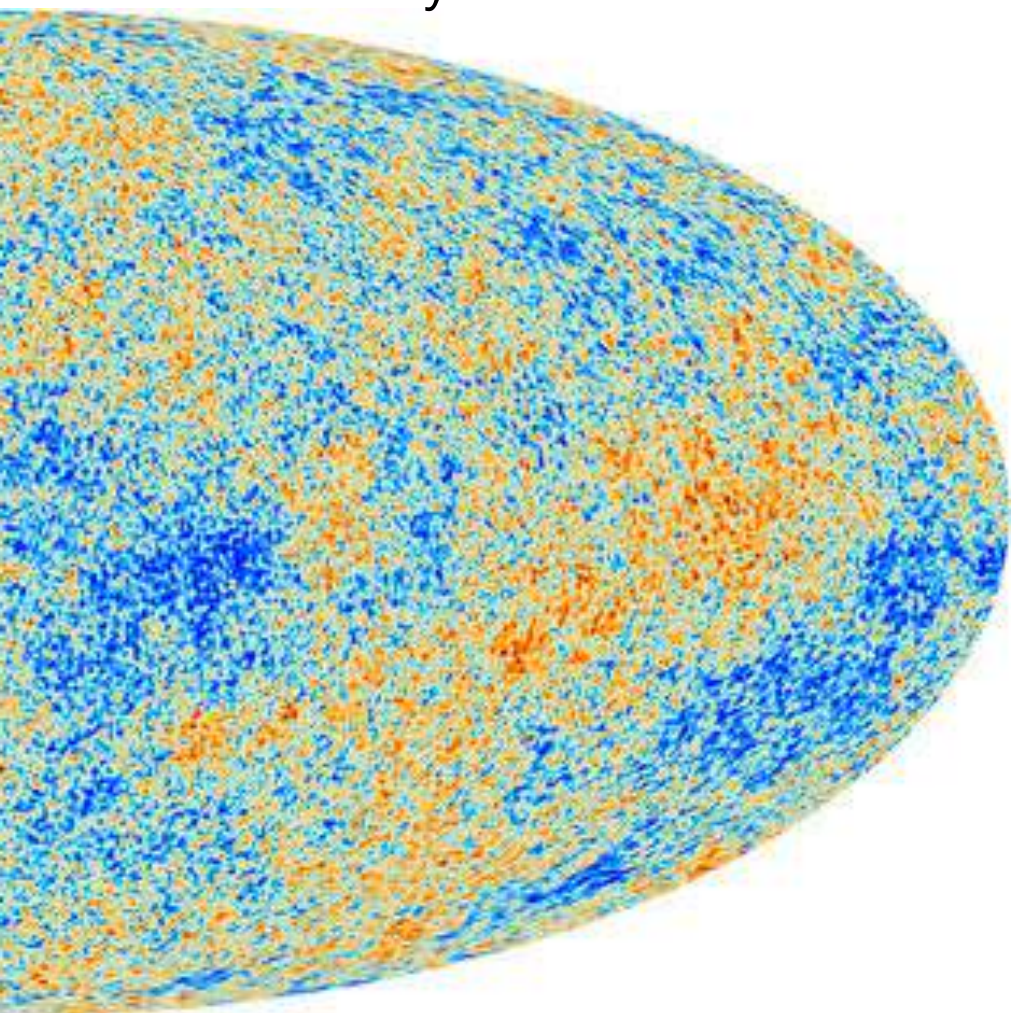


Figure 1. Relation between the half-mass radius of stellar distribution in galaxies of different stellar masses (spanning more than eight orders of magnitude in stellar mass) and morphological types and inferred virial radius of their parent halos, R_{200} , defined as the radius enclosing overdensity of $200\rho_{\text{cr}}$, and estimated as described in Section 2. The red and orange symbols and lines show early-type galaxies, while blue and cyan symbols and line show late-type galaxies, as indicated in the figure legend (see Sections 3 and 4.1 for details). The gray dashed line shows linear relation $r_{1/2} = 0.015 R_{200}$ and dotted lines are linear relations offset by 0.5 dex, which approximately corresponds to the 2σ scatter $2\sigma_{\ln\lambda} \approx 1.1$ expected for dark matter halos.

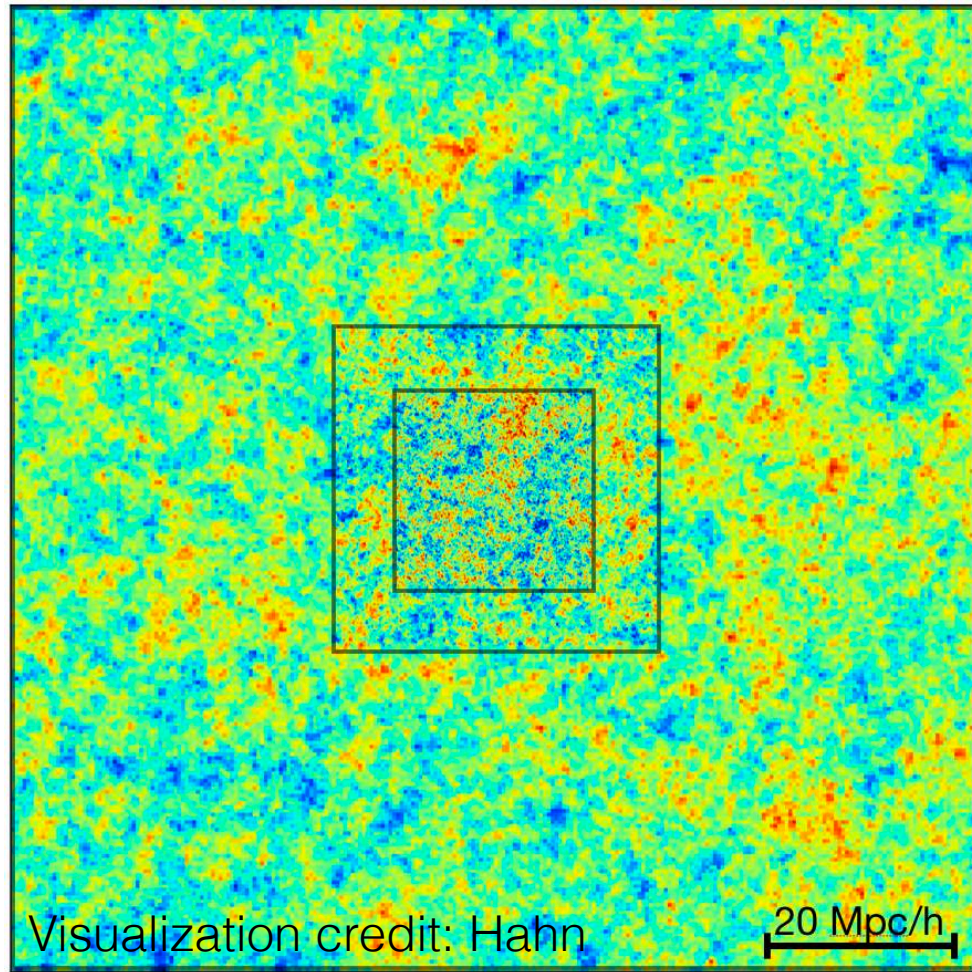
Cosmological N -body simulations
and
the structure of dark matter halos
(not covered in class)

Initial conditions for cosmological simulations

Microwave sky



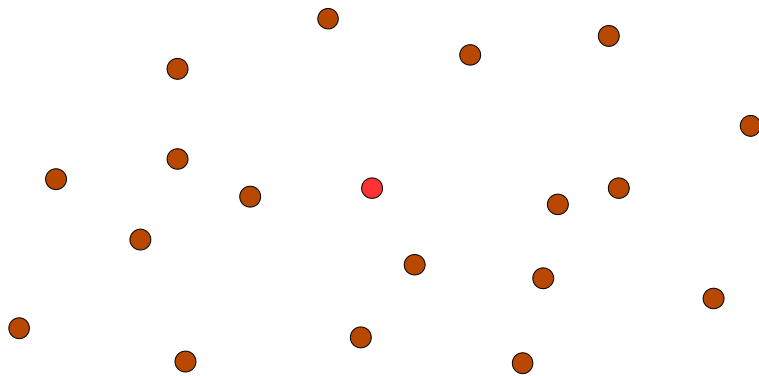
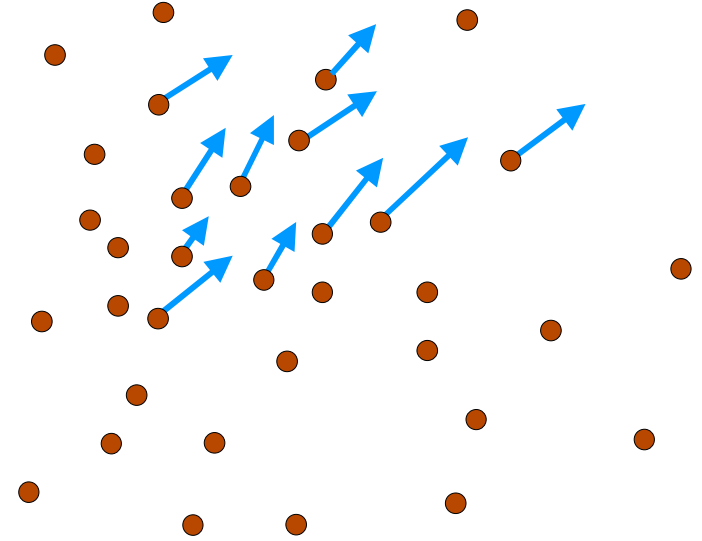
Simulation ICs



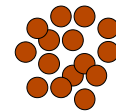
Gaussian random field filtered with "transfer function" to model early Universe physics (photon-baryon interactions)

N -body simulations

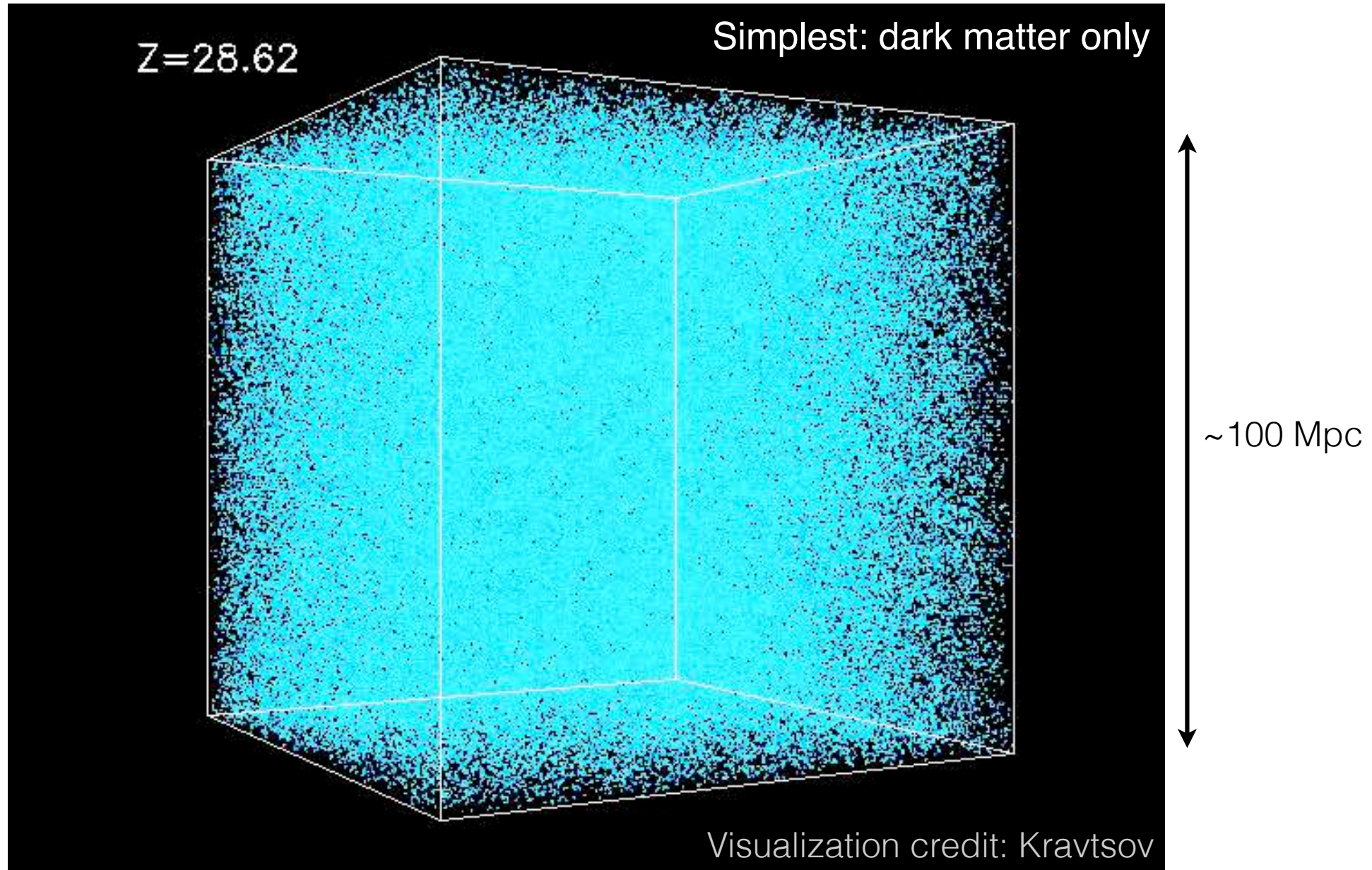
- Discretize mass with N particles
 - ▶ in cosmology, usually tree or particle-mesh methods to solve Poisson's equation
- Naturally adaptive in cosmology



collapse →



Gravity amplifies primordial fluctuations, forms structures



Density peaks (dark matter halos) are the sites of galaxy formation

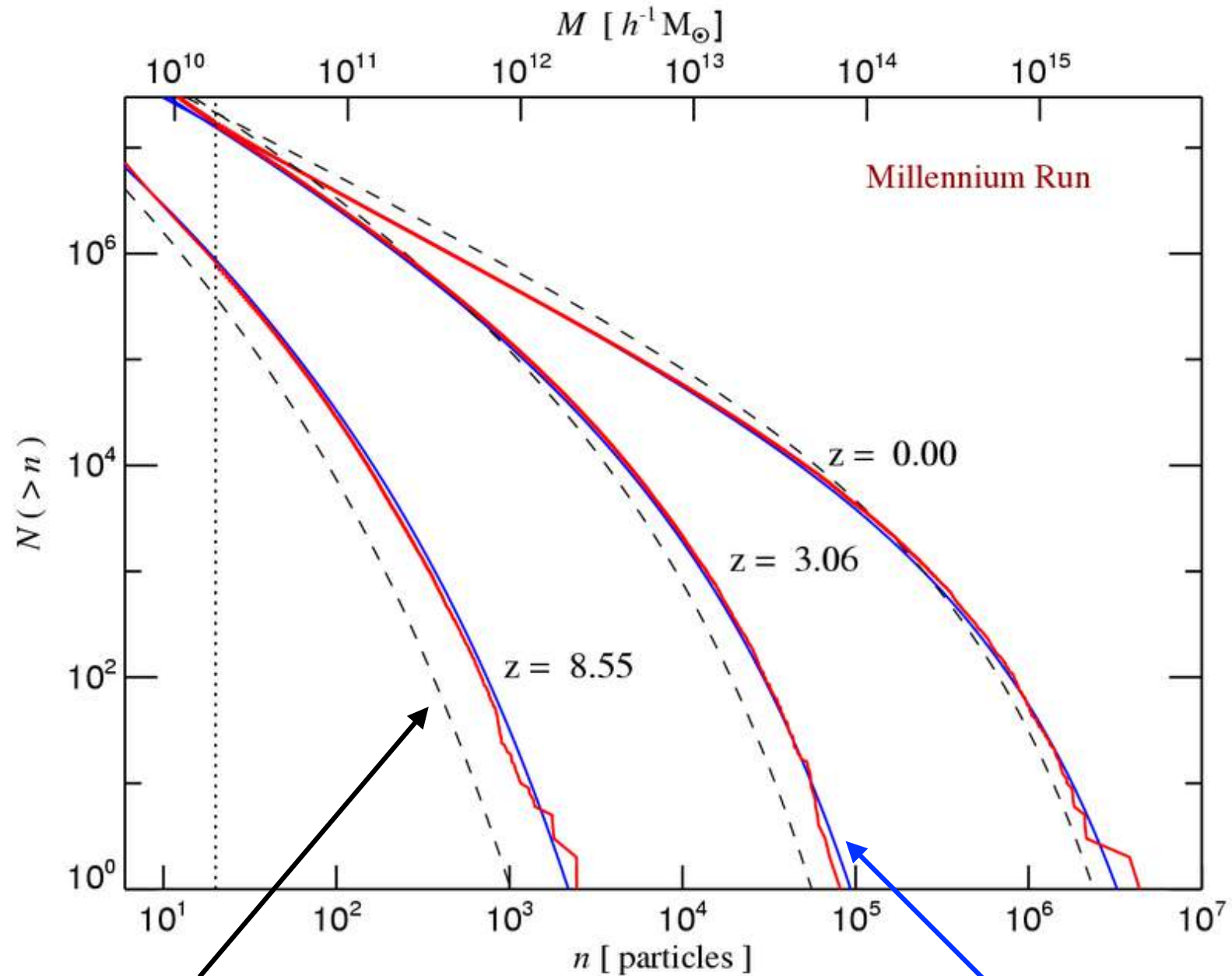
Millennium simulation ($z=0$ fly through)



10^{10} particles, $500 h^{-1}$ Mpc

Springel+05

Dark matter halo mass function



Press-Schechter analytic theory

Seth-Tormen fit

(Nearly) universal dark matter halo profile

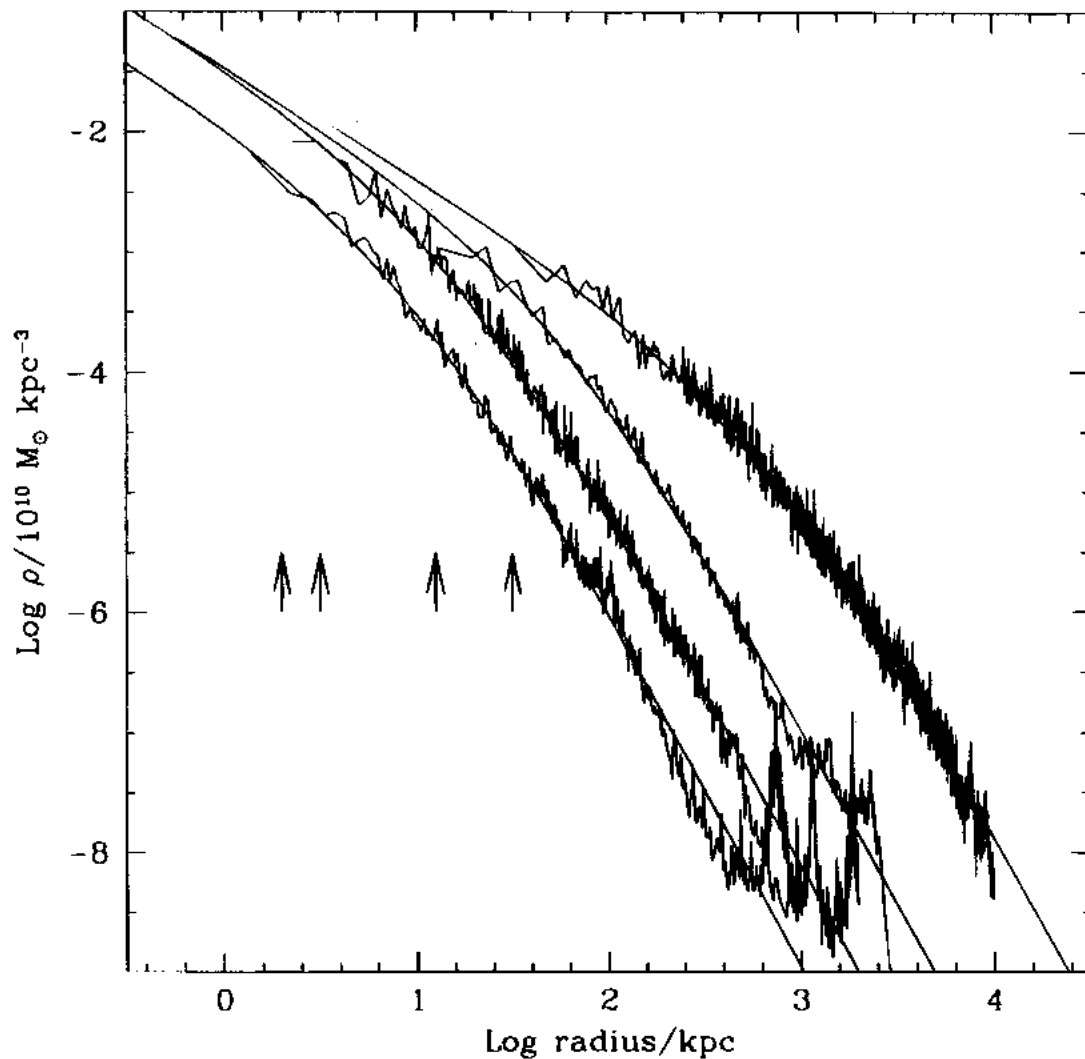


FIG. 3.—Density profiles of **four halos spanning 4 orders of magnitude in mass**. The arrows indicate the gravitational softening, h_g , of each simulation. Also shown are fits from eq. (3). The fits are good over two decades in radius, approximately from h_g out to the virial radius of each system.

NFW profile

$$\frac{\rho(r)}{\rho_{\text{crit}}} = \frac{\delta_c}{(r/r_s)(1+r/r_s)^2}$$

$$\delta_c = \frac{200}{3} \frac{c^3}{[\ln(1+c) - c/(1+c)]}$$

$$r_s = r_{200}/c$$

fits halos of all masses in N -body sims

Concentration correlates with halo mass

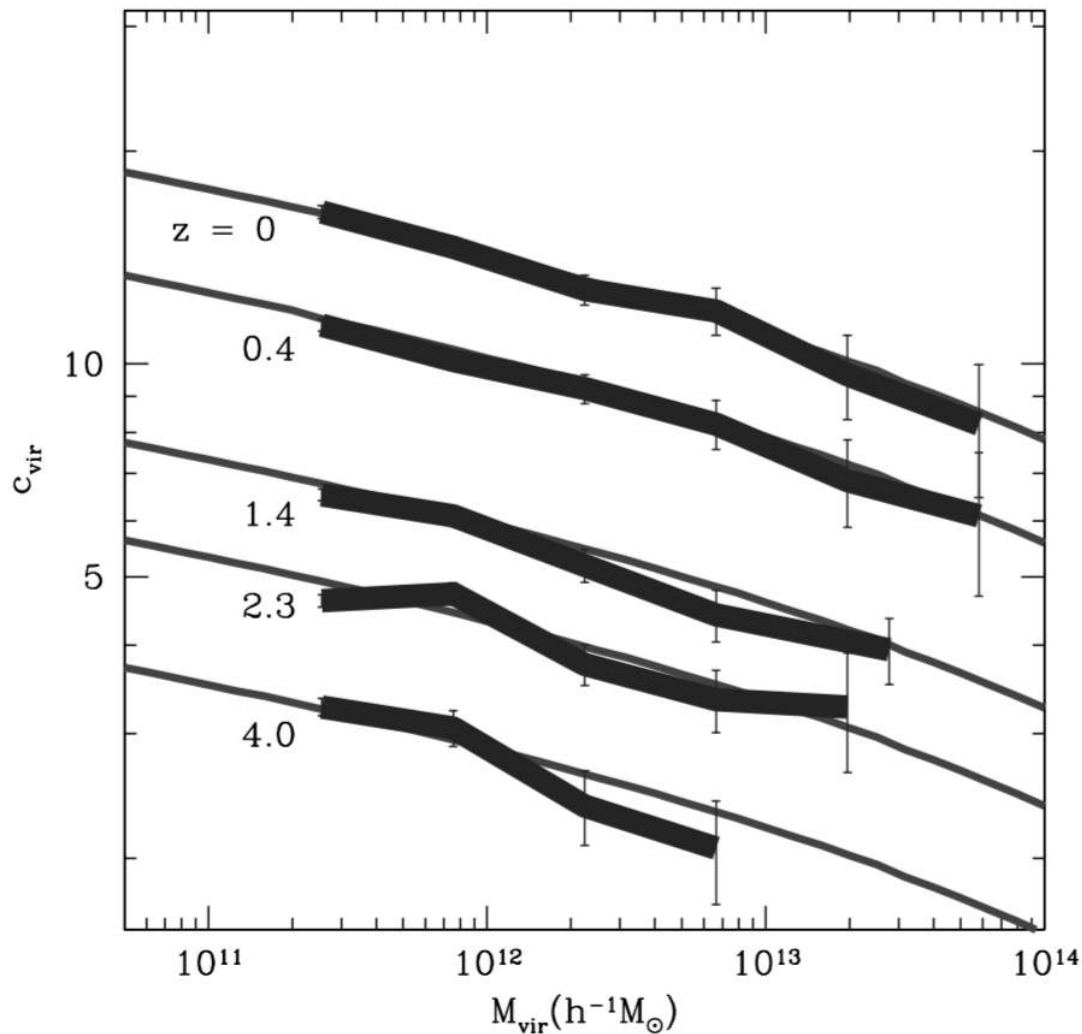


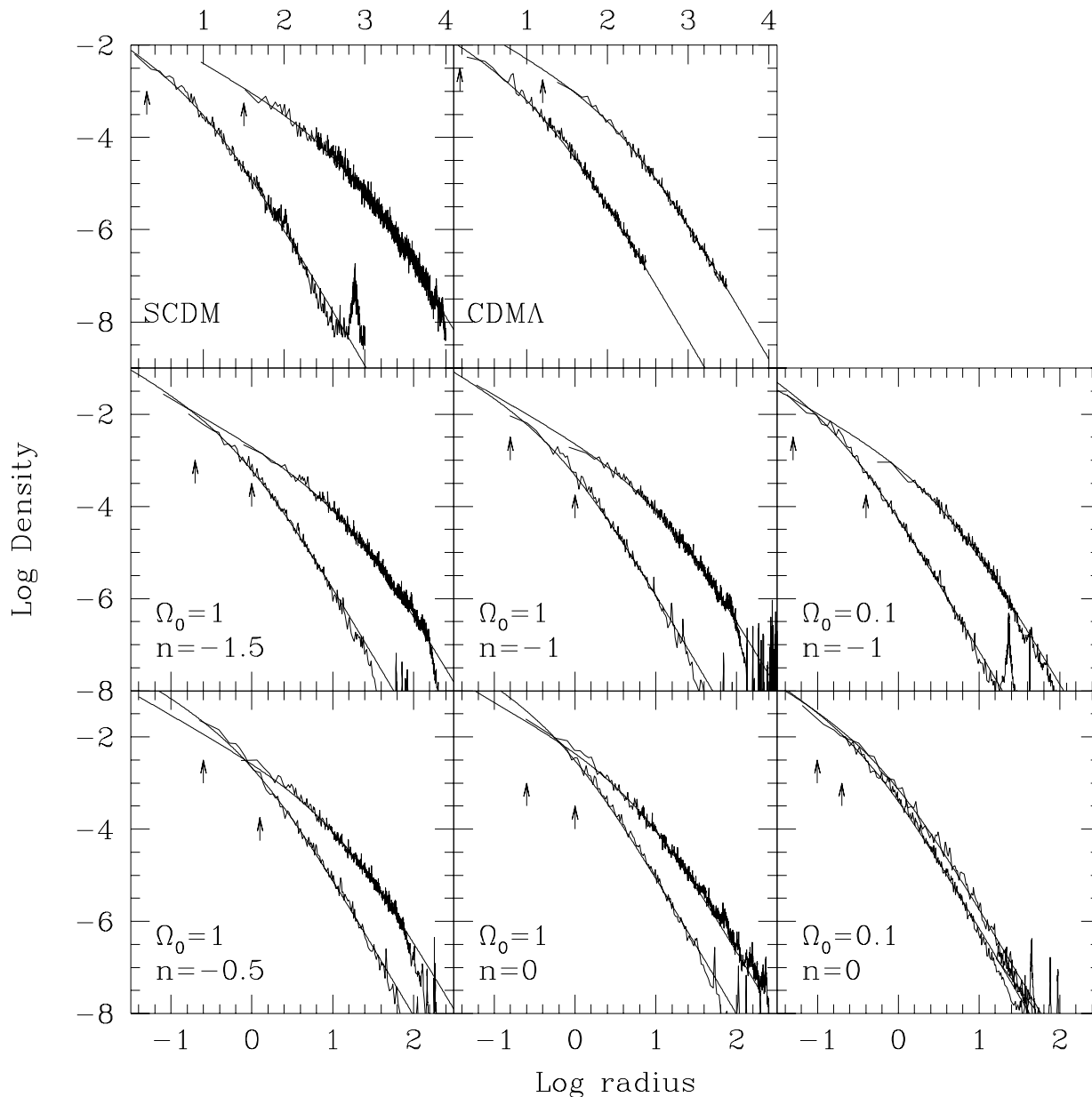
Figure 10. Median c_{vir} values as a function of M_{vir} for distinct haloes at various redshifts. The error bars are the Poisson errors due to the finite number of haloes in each mass bin. The thin solid lines show our toy model predictions.

Dark matter halo profiles form an (approximately) two-parameter family (M_{200} and z)

[Historical note: original NFW paper focused on $z=0$ so said ‘one-parameter’ family]

$$c \approx 15 \left(\frac{M_{200}}{10^{12} M_{\odot}} \right)^{-0.2} (1+z)^{-1}$$

NFW profile is a generic outcome of CDM models

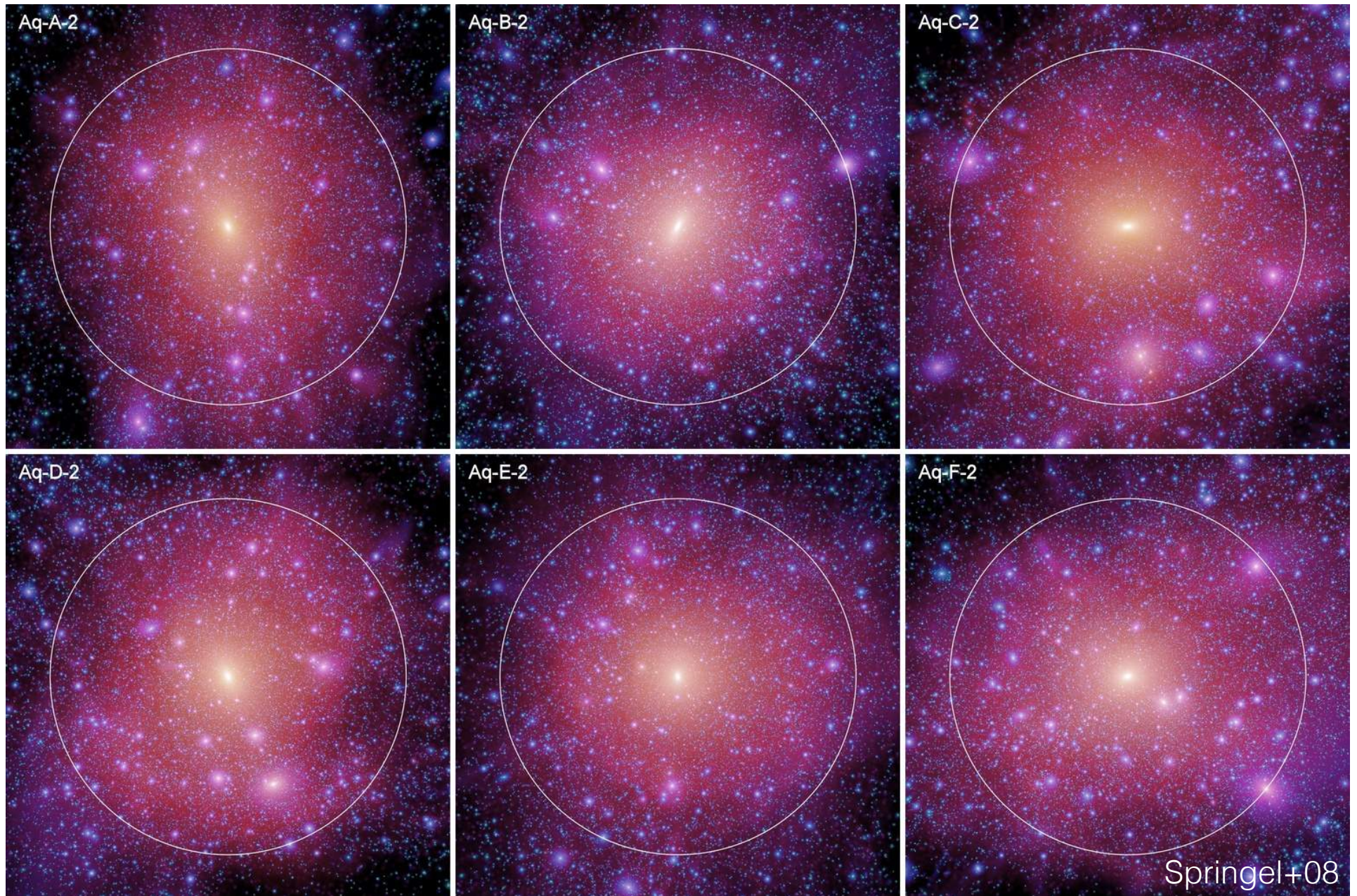


In CDM simulations,
 NFW emerges
 independent of
 cosmological
 parameters (e.g.,
 $\Omega_m \equiv \Omega_0$) and power
 spectrum of initial
 conditions (spectral
 index n)

Still not fully understood

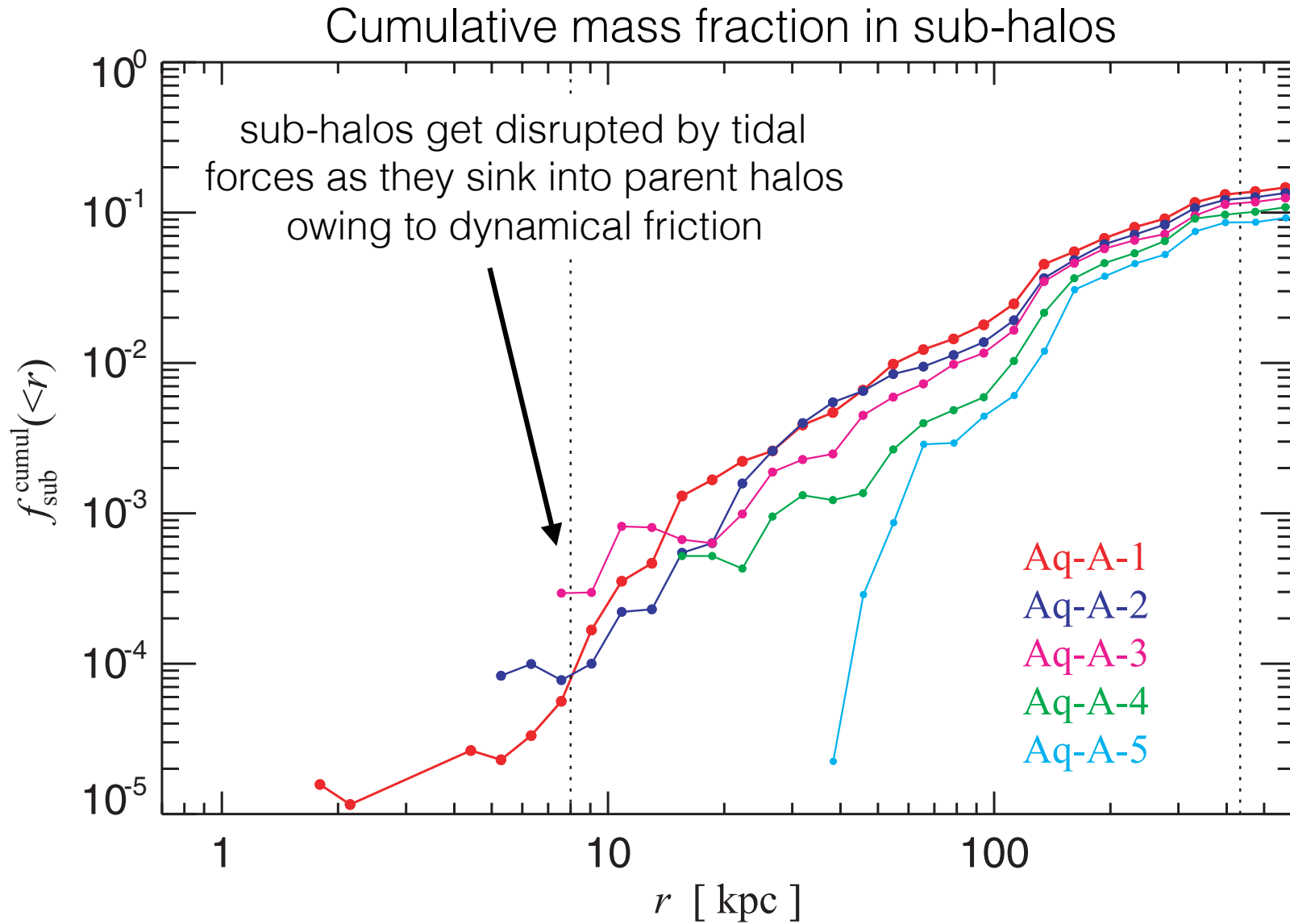
FIG. 2.—Density profiles of one of the most massive halos and one of the least massive halos in each series. In each panel, the low-mass system is represented by the leftmost curve. In the SCDM and CDMA models, radii are given in kiloparsecs (*scale at top*), and densities are in units of $10^{10} M_{\odot} \text{ kpc}^{-3}$. In all other panels, the units are arbitrary. The density parameter, Ω_0 , and the value of the spectral index, n , are given in each panel. The solid lines are fits to the density profiles using eq. (1). The arrows indicate the value of the gravitational softening. The virial radius of each system is in all cases 2 orders of magnitude larger than the gravitational softening.

Dark matter substructure: Aquarius simulations



$6 M_h \sim 10^{12} M_{\text{sun}}$ (zoomed in) halos, ultra-high res. (up to 10^9 particles within R_{vir})

Dark matter substructure fraction



≈10% halo mass in sub-halos